Journal of King Saud University – Science 31 (2019) 913–930

Contents lists available at ScienceDirect

Journal of King Saud University – Science

journal homepage: www.sciencedirect.com

Original article

Optimization of protein yields by ultrasound assisted extraction from *Eurycoma longifolia* roots and effect of agitation speed

Husam Eldin Elhag Abugabr Elhag [a], Aishath Naila [a], Abdurahman H. Nour [a], Azilah Ajit [a], Ahmad Ziad Sulaiman [a,*], Badhrulhisham Abd Aziz [b]

[a] Faculty of Chemical and Natural Resources Engineering, Universiti Malaysia Pahang, Lebuhraya Tun Razak, 26300 Gambang, Pahang Darul Makmur, Malaysia
[b] Faculty of Bio-Engineering & Technology, Universiti Malaysia Kelantan, Jeli Campus, Locked Bag No. 100, 17600 Jeli Kelantan, Malaysia

ARTICLE INFO

Article history:
Received 11 October 2017
Accepted 10 May 2018
Available online 19 May 2018

Keywords:
Eurycoma longifolia
Optimization
Protein
RSM
Ultrasound
Agitation speed
Predictive models

ABSTRACT

The traditional ways of protein extraction is disadvantageous from both economic and environment perspective. In this study, ultrasonic assisted extraction, UAE technique was used for the first time for the optimization process of extracting proteins from *Eurycoma longifolia* roots. The experiments demonstrated the successful effect of applying eccentric agitation with UAE to provide a combination of agitation and sonication to extract the proteins in short extraction times. Central composite design (CCD) was used to optimize the Ultrasonic-assisted extraction of proteins from roots of *Eurycoma longifolia* by water. Response surface methodology (RSM) was employed to investigate the effects of five independent variables; particle sizes (A), extraction temperatures (B), agitation speeds (C), amplitude (D) and duty cycle (E). The second enhanced model (Y_2) prevailed to be more efficient in protein recovery with optimum conditions of A: 0.022 ± 0.022 mm, B: 49 °C, C: 1314 rpm, D: 9 W and E: 63% UI: 2.94 W·cm^{-2} was 9.543 ± 0. 946%. High agitation speed didn't only affect the solvent properties, the diffusion of the solutes from the particles, cooling the extraction temperature, but influenced the distribution of cavitation bubbles and their impact on the solid particles. UAE was found to minimize the extraction of the same amount by conventional extraction 7-fold times. The results obtained in this study have exposed the capability of ultrasonic assisted extraction, UAE technology in extraction of protein from *E. longifolia* roots. Further works are nevertheless required to provide deeper understanding of the mechanisms involved to facilitate the development of optimum system applicable to the industry.

1. Introduction

Eurycoma longifolia (Tongkat Ali Jack) is a well-known plant in treating erectile dysfunction, increasing sexual desire, enhancing muscular ability (Low and Tan, 2007) and improving spermatogenesis (Wahab et al., 2010). This plant is traditionally consumed by the decoction of its roots (Nordin, 2014) and encouraged the production of various water-based commercial products (Mohd Effendy et al., 2012; Mohamed et al., 2015). These products have been usually standardized by the yield of the major metabolite eurycomanone (Abdul-Aziz et al., 2014; Abugabr Elhag et al., 2016) at optimum conditions of 100 °C and 400 rpm (Mohamad et al., 2010, 2013).

However, it is known that conventional procedures suffered from shortcomings of extended durations and high temperatures (Spigno et al., 2007; Stamatopoulos et al., 2013). Therefore the application of green extraction processes such as ultrasonic-assisted extraction (UAE) is encouraged to improve the extraction process intensifications and extraction rates with shorter extraction durations and less energy consumption (Chemat et al., 2017a; Esclapez et al., 2011; Jacotet-Navarro et al., 2016). UAE is a green extraction technology which is known to increase the yields of targeted phytochemicals (Shirsath et al., 2012) with minimization of product wastes, maintenance costs (Chemat et al., 2017a) and reduction of environmental impacts (Chemat et al., 2017b).

* Corresponding author.
E-mail addresses: abrahman@ump.edu.my (A.H. Nour), azilahajit@ump.edu.my (A. Ajit), ziad@ump.edu.my (A.Z. Sulaiman), badhrulhisham.a@umk.edu.my (B.A. Aziz).
Peer review under responsibility of King Saud University.

Production and hosting by Elsevier

https://doi.org/10.1016/j.jksus.2018.05.011
1018-3647/

The mechanisms of UAE depend on the generation of cavitation bubbles that enlarge during the rarefaction cycles and decrease during the compression cycles (Veillet et al., 2010). After reaching critical sizes during the compression cycles, the cavitation bubbles collapse and the high generated temperatures and pressures create microjets that develop shockwave damages on the solid–liquid interface (Pingret et al., 2013) and penetrate adjacent solid surfaces (Leonelli and Mason, 2010) such as plant cell walls (Veillet et al., 2010).

Even though the implementation of UAE to extract natural products has been widely investigated (Aguiló-Aguayo et al., 2017; Caleja et al., 2017; Fang et al., 2016; Ghitescu et al., 2015; Kadam et al., 2015; Kumari et al., 2017; Mane et al., 2015; Sousa et al., 2016), few studies have investigated *E. longifolia* extraction by UAE. These studies focused on screening eurycomanone (Mohd Zaki et al., 2015), isolating bioactive compounds (Park et al., 2014) and evaluating antibacterial activities (Danial et al., 2013). Water extractable proteins in *E. longifolia* roots were scarcely investigated even though they are considered important biochemical markers (Malaysian Standard, 2011). Few studies focused on protein concentrations (Chua et al., 2014) or their role as biomarkers in authenticating and profiling *E. longifolia* products (Chua et al., 2013; Nurhanan et al., 2004). Total concentrations of proteins were investigated by exhaustive conventional methods using prepared standardized extractions (Shuid et al., 2012), water extracts (Harun et al., 2015) or organic solvents (Khanam et al., 2015). However, within the numerous studies of protein extraction and recovery from various sources by UAE (Higuera-Barraza et al., 2017; Jiang et al., 2017; Li et al., 2018; Lupatini et al., 2016; Malik et al., 2017; Preece et al., 2017; Roselló-Soto et al., 2015; Wang et al., 2017; Yu et al., 2016), the optimization of UAE in protein extraction from *E. longifolia* roots was not investigated.

Response surface methodology (RSM) is collection of mathematical and statistical techniques that are used to optimize, improve and develop functional relationships between the process variables and their interactive effects on response variables. The regression analyses were designed to predict the values of the dependent variables based on the controlled values of the input variables (Myers et al., 2016).

This study was established to investigate the optimization of protein extraction from *E. longifolia* roots by UAE accompanied with mechanical agitation. The experimental set was repeated with a higher range of agitation speeds to study the effect of high agitation speed on the efficiency of the ultrasound regiments in protein extraction. Mathematical models for both sets were established to generate quadratic and enhanced models to predict the optimized conditions for protein extraction.

2. Materials and methods

2.1. Sample preparation for extraction

Dried roots of *E. longifolia* were obtained at University Malaysia Pahang (UMP) under the research Grant RDU 161,601 and RDU 160801. The roots were air dried and pulverized by a SZ-1000A-3 grinder and sieved by a calibrated granulometric sieve GB/T6003.1-1997 to obtain the desired particle sizes (Table 1).

2.2. Reagents and equipment

All reagents were purchased from Merck (Germany), Sigma Aldrich (USA) and Fisher scientific (UK) and were analytical grade. The conventional part of the extraction was performed by a IKA® MAG HS7 hot plate magnetic stirrer while the sonication part was preformed by a QSonica ultrasonic processor Q700 (700 watts, 20 kHz) with a replaceable flat tip ultrasonic probe (length: 127 mm, diameter: 12.7 mm) made from titanium alloy due to its low mass and high rigidity. Bovine Serum Albumin (BSA) was used to establish the standard curve. Concentrations of proteins were investigated using a Hitachi U 1800 UV/VIS spectrophotometer (UK). Ultrapure water was provided by Milli-Q ultrapure water system.

2.3. Total extractable protein

The concentration of the proteins was estimated by applying a multistep extraction process (Harun et al., 2015) with modifications. Dried pulverized roots (10 g) with particle size (diameter 0.071 ± 0.017 mm) were macerated with 250 ml distilled water at 50 °C and agitation speed 400 rpm for 4 h in a 500 ml beaker. At the end of the process the extracts were separated by filtration in a 1L Scotch bottle and preserved in 4 °C and the step was repeated 4 times on the same powdered roots. The accumulative extraction was tested for the total protein content by Lowry method (Lowry et al., 1951; Waterborg, 2009).

2.4. Extraction procedure

This study applied UAE for protein extraction from *E. longifolia* roots by a combination of five factors, namely particle size (*A*), temperature (*B*), agitation speed (*C*), amplitude (*D*) and duty cycle (*E*). The first set of the agitation speed ranged from 200 to 800 rpm. The experiments were repeated with a higher range of agitation speeds from 800 to 1500 rpm to investigate the effect of high agitation speeds on the efficiency of UAE. Each extraction procedure was established in a 250 ml beaker. The IKA® MAG HS7 hot plate provided the designated heat and agitation speed and the temperature was observed with a thermometer until constancy of the selected temperature was reached. Eccentric agitation by a magnetic stirrer was adopted for the setup of the experiment to avoid the undesired vortex phenomenon in mixing processes (Alvarez et al., 2002; Montante et al., 2006). With the decline of the vortex phenomenon, the ultrasonic probe was located near the center of the water surface (Fig. 1). The tip of the probe was dipped 30 mm under the surface of the solvent through careful measurements and rehearsals. Amplitude (*D*) and duty cycle (*E*) were adjusted in advance. Sonication started once the powdered sample (5 g) was added to the water with constant liquid to sample ratio

Table 1
Levels of variables employed for the construction of Central Composition Design (CCD).

	Variables	Levels				
		−1.322	−1	0	1	1.322
A	Particle size ((mm))	0.022	0.071	0.223	0.375	0.424
B	Extraction temperature (°C)	45	50	65	80	85
C	Agitation speed (200–800 rpm)	103	200	500	800	897
	Agitation speed (800–1500 rpm)	687	800	1150	1500	1613
D	Amplitude (W)	1	2	6	10	11
E	Duty cycle (%)	37	40	50	60	63

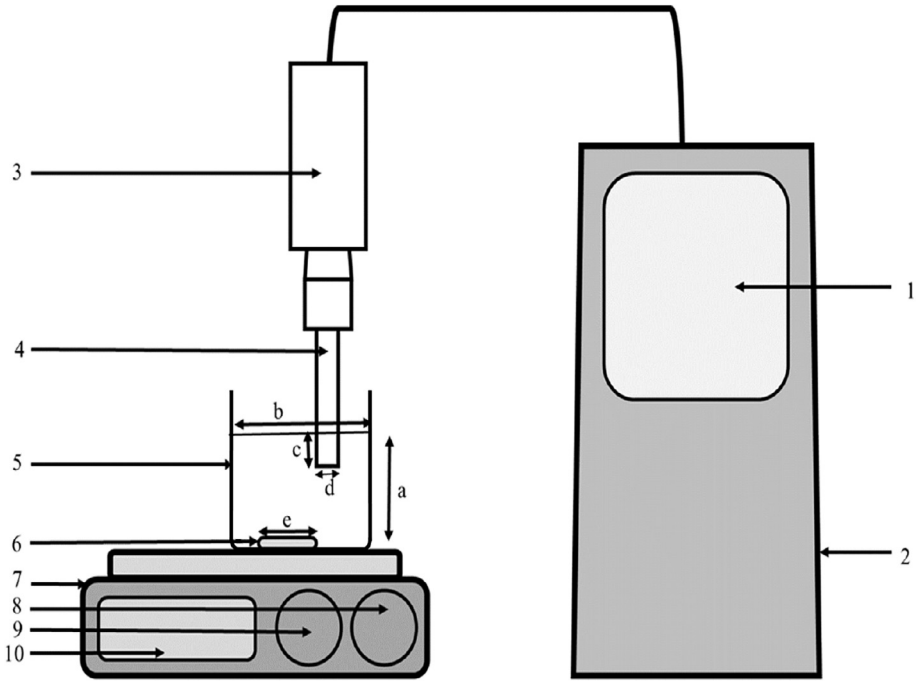

Fig. 1. Experimental setup of UAE; 1. Sonicator screen 2.Sonicator 3.Probe 4.Probe tip 5.Unbaffled vessel (Beaker) 6.Stirring rod 7. Hot plate 8.Stirring adjustment knob 9. Temperature adjustment knob 10. Hot plate screen.

(40:1). The sonication time was fixed to 5 min. Extracts were immediately filtered by Whatman filter paper No. 1 and preserved at −20 °C. All experiments for both sets were triplicated and carried out randomly to minimize any effect of extraneous factors on the observed responses.

2.5. Protein isolation and yield (%)

Proteins were recovered by the acetone precipitation method (Rinas and Jones, 2015; Tazi and Jayawickreme, 2016). Four mL of cooled acetone (−20 °C) was added to 1 mL extract in an acetone-compatible tube and vortexed for 60 min. Then the mixture was centrifuged for 10 min at 12,000 g and the supernatant was disposed carefully so the protein pellet would not be dislodged. The step was repeated twice to remove any interfering substance before the acetone was allowed to evaporate in room temperature with precaution of not over-drying the pellet. The pellet then was dissolved in 1 mL of ultrapure water and vortexed. Protein concentrations in all samples and standard solutions were determined by Lowry method (Lowry et al., 1951; Waterborg, 2009). Yields (%) of proteins were expressed by their percentages of the extracted proteins weights (g) to the plant sample weight (g) according to (Eq. (1)):

$$Y_A(\%) = \frac{B \times C}{D} \times 100\% \quad (1)$$

where Y is the yield of protein yields, A corresponds to the experimental set 1 or 2, B is the concentration ($g{\cdot}mL^{-1}$), C is the whole volume of extract (mL), *and* D is the weight of the raw sample (g).

2.6. Measurement ultrasonic intensity (UI)

The level of energy introduced into the system was expressed by the dissipated ultrasonic power (P) in the water (Eq. (2)). The ultrasonic power was further employed to measure the ultrasonic intensity (UI) (Eq. (3)) (Boukroufa et al., 2015; Carail et al., 2015; Pingret et al., 2012; Sicaire et al., 2016).

$$P = m \cdot C_p \cdot \frac{dT}{dt} \quad (2)$$

$$UI = \frac{4P}{\pi D^2} \quad (3)$$

where P is the ultrasonic power (W), m is the water mass (g), C_p is the specific heat of the water at constant pressure (4.184 J g^{-1} °C^{-1}) and (dT/dt) is the initial rate of change of temperature over time (°C s^{-1}) which was determined by fitting temperature change obtained by a thermometer against sonication time, UI is the ultrasonic power intensity ($W{\cdot}cm^{-2}$), D is the diameter (cm) of the tip of the probe.

2.7. Experimental design and statistical analysis

To investigate the performance of UAE of protein yields, response surface methodology (RSM) was employed in Minitab 17 software (Minitab, 2014) to achieve maximal data about the extraction process from a minimal number of experiments with a circumscribed central composite design (CCCD). The design optimized the process with three levels (−1, 0, +1) and star points ($\alpha = \pm 1.322$) from the center base. This permitted the fitting of the second order model (Eq. (4)) for the effect of the independent variables and their interactions on the protein yields (Myers et al., 2016).

$$Y = b_0 + \sum_{n-1}^{n} b_n x_n + \sum_{n=1}^{n} b_{nn} x_n^2 + \sum_{n \neq m=1}^{n} b_{nm} x_n x_m \quad (4)$$

where Y is the predicted response variable of the yield (%) for proteins; b_0 is the average response obtained at the replicated center point (0, 0, 0, 0) of the CCCD; b_n, b_{nn} and b_{nm} are the linear, quadratic and interaction regression coefficients, respectively.

The lower, middle and higher coded values for all factors were −1, 0 and 1. The variables were coded according to (Eq. (5)):

$$X_i = \frac{x_i - \bar{x}_i}{\Delta x_i} \quad (5)$$

where the X_i is the coded value, x_i is the real value of the independent variable, $\bar{x}_i$ is the real value of an independent variable at the center point and Δx_i is the step change.

Statistical analyses were employed to determine the standard error of regression (S), coefficient of determination (R^2), adjusted coefficient of determination (R^2_{adj}) and predicted coefficient of determination (R^2_{pred}). Adequacy of the models were determined by the p values of the lack of fit tests at significant level of 95% ($p > 0.05$) (Myers et al., 2016). The 3D Surface plots were generated in Design Expert (Version 7.1.6; Stat- Ease Inc, Minneapolis, MN, USA) for better visualizations of the interactive effects between the extraction factors.

2.8. Enhanced models

Enhanced models for both sets were obtained by eliminating the non-significant terms ($p > 0.05$) from the full quadratic equations (one-by-one). The remaining significant terms expressed these enhanced models with more accuracy in predicting the protein yields (%) and determining the optimized conditions of the sonication processes.

2.9. Scanning electron microscopy (SEM)

Surface morphology of the untreated and UAE treated powdered roots was examined by a Hitachi-TM3030 tabletop scanning electron microscope (Hitachi High Technologies America Inc., USA). The samples were fixed on specimen holders and sputtered with gold then scanned under high vacuum conditions with an accelerating voltage of 15.0 kV and a working distance of 6.8–7.2 mm.

3. Results and discussion

3.1. Experiment setup and main effects of extraction factors

Extraction is the first key step in isolating natural compounds from plants (Samaram et al., 2015), therefore the performed extraction of the targeted metabolite should be considered by efficiency and reproducibility beside waste reduction awareness of climate change (Chemat et al., 2017a). In this study, the process was influenced by the UAE regiments and factors including frequency, ultrasonic intensity, temperature and extraction time (Shirsath et al., 2012) in addition to the mechanical agitation that created combined effects with the solvent volume and temperature (Wang and Weller, 2006). Ultrapure water was used as the extraction solvent this study due to safety and the high solubility of proteins in water (Pace et al., 2004); the eccentric agitation illustrated high suitability in the extraction process as it caused various alterations in the flow structure of the solvent (Alvarez et al., 2002; Montante et al., 2006) resulting in the formation and maintenance of homogeneous suspensions of particles to obtain flocculation and collision between particles and solvent (Varzakas and Tzia, 2014).

Pareto charts for the two sets of agitation revealed that the most common and effluent factor is the particle size (A); other factors differed between the two sets. Temperature (C) was noticed to be significant only with the application of high agitation speeds while agitation speed was only significant with the application of low agitation speed range (Fig. 2). The main effects of the extraction factors are illustrated in (Fig. 3). Differences in the main effects revealed that high agitations speeds increased the effect of all factors with various alterations in the behavior of some factors.

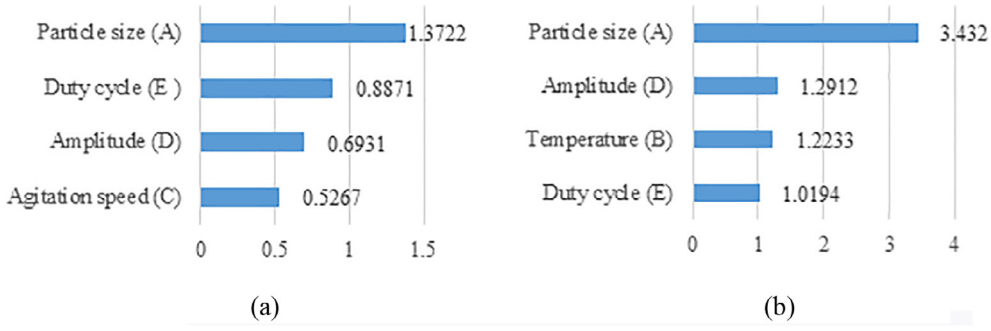

Fig. 2. Pareto charts for significant factors for (a) Y_1 and (b) Y_2.

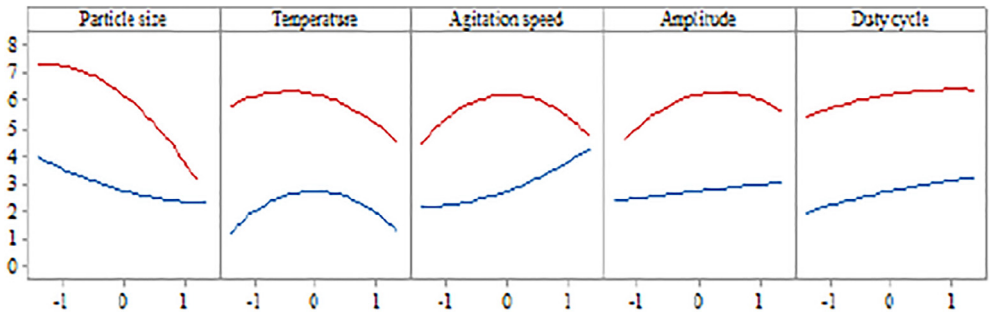

Fig. 3. Main effects extraction factors on the protein yields Y_1 (blue dashes) and Y_2 (red line).

3.2. Total proteins concentration in E. longifolia roots

The total amount of water soluble proteins was obtained by adopting the multistep process (Harun et al., 2015) with the above mentioned modifications in (2.3.). The average amount of water soluble proteins yields from 3 samples (10 g) was 15.957 ± 0.381% at the end of the fourth step. This was with agreement with Chua et al. (2013) who stated that the concentrations of *E. longifolia* proteins ranged between 15.5 and 39.3% according to geographical origins of the plant.

3.3. Fitting of models and statistical analyses

The experimental values of the protein yields were employed by CCCD to generate full quadratic models to calculate predicted yields (%). Enhanced models for both sets were established by eliminating the terms with no significant effect ($p > 0.05$) from the quadratic models (one-by-one) and they were employed to calculate more accurate protein yields (%) (Table 2).

Table 2
Experimental design of the CCCD, the estimated Ultrasound intensity and protein yields (%) Y_1 and Y_2.

No.	Extraction factors					Yield of proteins (%) (Y_1)				Yield of proteins (%) (Y_2)			
	A (r = mm)	*B* (°C)	*C* (rpm)	*D* (W)	*E* (%)	UI_1 (W·cm^{-2})	Exp. (%)	Pred. (%)	Enh. (%)	UI_2 (W·cm^{-2})	Exp. (%)	Pred. (%)	Enh. (%)
1	−1	−1	1	1	1	2.95	6.619 ± 0.363	6.481	6.561	3.70	8.578 ± 1.093	8.348	7.833
2	1	−1	−1	1	1	0.31	1.171 ± 0.069	1.402	1.337	2.95	3.037 ± 0.725	2.798	3.115
3	1	1	1	−1	−1	1.38	1.739 ± 0.709	1.602	1.544	1.06	0.452 ± 0.608	0.776	0.281
4	1	1	1	1	1	2.30	2.212 ± 0.339	1.962	2.049	2.55	0.322 ± 0.392	0.460	0.485
5	1	−1	−1	−1	−1	0.61	0.872 ± 0.027	0.837	0.917	1.69	1.660 ± 0.759	1.398	1.427
6	0	0	0	0	0	1.41	2.644 ± 0.350	2.758	2.743	2.53	6.391 ± 1.815	6.246	6.223
7	−1	−1	1	−1	−1	1.40	2.623 ± 0.206	2.954	2.888	1.70	4.096 ± 0.349	4.600	4.645
8	1	1	−1	−1	1	0.11	2.638 ± 0.342	2.567	2.506	1.50	1.561 ± 0.558	1.592	1.735
9	−1	−1	−1	−1	1	0.04	1.983 ± 0.059	2.026	1.957	1.98	4.763 ± 0.792	4.720	4.595
10	0	0	0	0	0	1.67	2.741 ± 0.270	2.758	2.743	2.53	6.672 ± 1.194	6.246	6.223
11	1	−1	1	1	−1	2.28	1.650 ± 0.013	2.023	1.955	2.20	1.315 ± 0.909	1.382	1.353
12	−1	1	−1	−1	−1	0.26	1.323 ± 0.066	1.199	1.286	1.38	3.032 ± 0.029	3.202	3.499
13	1	−1	1	−1	1	1.68	2.062 ± 0.834	2.310	2.390	1.58	2.309 ± 0.572	2.107	2.553
14	1	1	−1	1	−1	0.54	1.199 ± 0.041	1.293	1.378	1.84	2.052 ± 0.650	2.272	2.019
15	−1	1	1	−1	1	1.50	3.244 ± 0.854	3.339	3.423	2.06	3.563 ± 0.661	3.934	3.777
16	−1	1	1	1	−1	1.84	4.391 ± 0.035	4.457	4.395	1.15	4.822 ± 1.241	5.050	5.561
17	−1	−1	−1	1	−1	0.16	0.702 ± 0.105	0.795	0.873	2.28	5.184 ± 1.313	4.808	4.895
18	0	0	0	0	0	1.65	2.655 ± 0.698	2.758	2.743	2.53	6.827 ± 1.375	6.246	6.223
19	−1	1	−1	1	1	0.12	2.385 ± 0.127	2.355	2.296	2.30	4.827 ± 1.045	5.154	5.203
20	0	0	0	0	0	1.65	2.693 ± 1.257	2.758	2.743	2.53	5.535 ± 1.787	6.246	6.223
21	−1	−1	1	1	−1	2.28	5.184 ± 0.593	4.938	4.869	2.20	6.165 ± 0.064	6.334	6.389
22	−1	1	−1	−1	1	0.14	2.145 ± 0.097	2.054	1.993	1.50	3.244 ± 0.387	3.400	3.459
23	1	1	1	1	−1	1.84	2.052 ± 0.097	1.980	1.919	1.15	0.814 ± 0.151	0.738	0.525
24	1	−1	−1	−1	1	0.51	2.207 ± 0.928	2.100	2.032	1.68	2.062 ± 0.545	2.272	2.871
25	1	1	1	−1	1	1.50	1.561 ± 0.028	1.589	1.673	2.06	0.147 ± 0.072	0.314	0.241
26	1	−1	1	−1	−1	1.69	1.660 ± 0.854	1.342	1.276	1.70	1.289 ± 0.253	1.148	1.109
27	1	1	−1	1	1	0.23	1.618 ± 0.230	1.566	1.507	2.30	2.212 ± 0.153	1.846	1.979
28	−1	−1	−1	−1	−1	0.55	0.124 ± 0.067	0.186	0.266	1.37	2.623 ± 0.886	3.038	3.151
29	0	0	0	0	0	1.86	2.842 ± 0.635	2.758	2.743	2.53	5.374 ± 0.211	6.246	6.223
30	−1	1	1	1	1	2.30	4.827 ± 1.076	5.015	5.102	2.55	5.449 ± 0.842	5.580	5.521
31	1	−1	−1	1	−1	0.92	0.431 ± 0.066	0.145	0.222	2.28	1.650 ± 0.761	1.740	1.671
32	0	0	0	0	0	1.75	2.751 ± 0.065	2.758	2.743	2.53	5.801 ± 0.366	6.246	6.223
33	1	1	−1	−1	−1	0.16	2.051 ± 0.031	2.289	2.377	1.38	1.739 ± 0.131	2.202	1.775
34	−1	−1	1	−1	1	1.98	4.763 ± 0.861	4.502	4.579	2.48	6.474 ± 0.643	6.430	6.089
35	1	−1	1	1	1	2.60	3.037 ± 0.695	2.990	3.070	2.93	2.673 ± 0.476	2.588	2.797
36	−1	1	1	−1	−1	1.38	3.032 ± 0.125	2.776	2.717	1.06	3.374 ± 0.116	3.588	3.817
37	0	0	0	0	0	1.89	2.991 ± 0.571	2.758	2.743	2.53	5.563 ± 0.941	6.246	6.223
38	−1	−1	−1	1	1	2.54	2.504 ± 0.123	2.630	2.564	2.60	6.619 ± 0.238	6.746	6.339
39	−1	1	−1	1	−1	0.02	1.624 ± 0.129	1.505	1.589	1.84	4.391 ± 1.355	4.772	5.243
40	0	0	0	0	0	1.71	2.837 ± 0.580	2.758	2.743	2.53	6.931 ± 0.764	6.246	6.223
41	0	1.322	0	0	0	1.83	1.149 ± 0.061	1.391	1.341	2.60	5.840 ± 0.649	4.619	4.539
42	0	0	0	0	0	1.73	2.766 ± 0.216	2.758	2.740	2.53	6.822 ± 0.438	6.246	6.223
43	0	0	−1.322	0	0	0.11	2.260 ± 0.193	2.149	2.095	2.13	4.772 ± 0.423	4.688	4.664
44	0	0	0	0	−1.322	1.05	1.894 ± 0.344	2.017	2.141	2.85	6.379 ± 0.294	5.481	5.758
45	0	0	0	0	0	1.44	2.534 ± 0.335	2.758	2.743	2.53	7.124 ± 1.063	6.246	6.223
46	0	0	0	−1.322	0	0.91	2.274 ± 0.137	2.411	2.418	1.69	5.244 ± 1.269	4.390	4.308
47	0	0	0	0	0	1.54	2.623 ± 0.823	2.758	2.740	2.53	6.449 ± 0222	6.246	6.223
48	−1.322	0	0	0	0	1.65	3.855 ± 0.295	3.924	3.870	2.63	8.293 ± 1.326	7.300	7.219
49	1.322	0	0	0	0	2.50	2.349 ± 0.285	2.338	2.283	2.53	2.172 ± 0.996	2.832	2.752
50	0	0	0	1.322	0	2.15	3.141 ± 0.596	3.061	3.067	2.45	5.181 ± 0.714	5.704	5.622
51	0	0	0	0	0	2.05	3.041 ± 0.079	2.758	2.743	2.73	5.653 ± 0.658	6.246	6.223
52	0	−1.322	0	0	0	2.26	1.585 ± 0.137	1.401	1.341	1.87	5.032 ± 0.704	5.918	5.837
53	0	0	1.322	0	0	2.48	4.073 ± 0.043	4.241	4.186	5.10	5.052 ± 0.349	4.805	4.664
54	0	0	0	0	1.322	2.29	3.288 ± 0.942	3.222	3.345	3.41	5.845 ± 0.732	6.409	6.687

A: Particle size radius (r = mm); *B*: Temperature (°C); *C*: agitation speed (rpm), *D*: Amplitude (W); *E*: Duty cycle (%); *UI*: Ultrasound intensity (Wcm^{-2}); UI_1: Ultrasound intensity at agitation speed range 200–800 rpm (Wcm^{-2}); UI_2: Ultrasound intensity at agitation speed range 800–1500 rpm (Wcm^{-2}).

3.3.1. Full quadratic models for protein yields (Y_1) and (Y_2)

The highest yield (7.619%) for Y_1 was obtained with the parameter values (A = 0.071 ± 0.017 mm, B = 50 °C, C = 800 rpm, D = 10 W and E = 60%). The full quadratic model for this yield (Eq. (6)) was:

$$\begin{aligned} Y_{1(\text{quadratic})}\ (\%) = {} & 2.7581 - 0.6002A - 0.0036B + 0.7910C \\ & + 0.2458D + 0.4553E + 0.2134A^2 \\ & - 0.7793B^2 + 0.2501C^2 - 0.0126D^2 \\ & - 0.0792E^2 + 0.1097A \cdot B - 0.5659A \cdot C \\ & - 0.3256A \cdot D - 0.1442A \cdot E - 0.2978B \cdot C \\ & - 0.0759B \cdot D - 0.2463B \cdot E + 0.3437C \cdot D \\ & - 0.0729C \cdot E - 0.0012D \cdot E \end{aligned} \quad (6)$$

The highest yield (8.578%) for Y_2 was obtained with the parameter values (A = 0.071 ± 0.017 mm, B = 50 °C, C = 1500 rpm, D = 10 W and E = 60%). The full quadratic model for this set was generated as in (Eq. (7)).

$$\begin{aligned} Y_{2(\text{quadratic})}\ (\%) = {} & 6.246 - 1.690A - 0.491B + 0.044C \\ & + 0.497D + 0.351E - 0.675A^2 - 0.559B^2 \\ & - 0.858C^2 - 0.686D^2 - 0.172E^2 + 0.160A \cdot B \\ & - 0.453A \cdot C - 0.375A \cdot D - 0.202A \cdot E \\ & - 0.294B \cdot C - 0.068B \cdot D - 0.371B \cdot E \\ & - 0.027C \cdot D + 0.037C \cdot E + 0.046D \cdot E \end{aligned} \quad (7)$$

Table 3
Significance of the regression coefficients associated with the various experimental factors.

Source	Y_1 (agitation speed 200 to 800 rpm)							Y_1 (agitation speed 800 to 1500 rpm)						
	SE coeff	SS	MS	Adj SS	Adj MS	F	p	SE coeff	SS	MS	Adj SS	Adj MS	F	p
intercepts	0.0559	73.51	73.68	73.971	81.10	0.000	0.001	0.0559	220.35	11.02	242.336	11.015	30.38	<0.001
A	0.0342	12.79	12.79	42.785	308.38	0.000	<0.001	0.101	101.34	101.34	101.428	101.428	279.73	<0.001
B	0.0342	0.0005	0.0005	0.001	0.0005	0.01	0.917	0.101	8.56	8.56	8.557	8.557	23.60	<0.001
C	0.0342	22.21	22.21	22.210	22.2105	535.72	<0.001	0.101	0.068	0.068	0.068	0.068	0.19	0.667
D	0.0342	2.14	2.14	2.144	2.1443	51.72	<0.001	0.101	8.77	8.77	8.766	8.766	24.18	<0.001
E	0.0342	7.36	7.36	7.359	7.3595	177.51	<0.001	0.101	4.38	4.38	4.385	4.385	12.09	0.002
A^2	0.0753	0.35	0.35	0.333	0.3326	8.02	0.008	0.223	3.56	3.56	3.327	3.327	9.17	0.005
B^2	0.0753	4.42	4.42	4.437	4.4369	107.02	<0.001	0.223	2.47	2.47	2.279	2.279	6.28	0.018
C^2	0.0753	0.48	0.48	0.457	0.4570	11.02	0.002	0.223	5.69	5.69	5.380	5.380	14.84	0.001
D^2	0.0753	0.0003	0.0003	0.001	0.0012	0.03	0.868	0.223	3.68	3.68	3.439	3.439	9.49	0.004
E^2	0.0753	0.042	0.042	0.046	0.0458	1.11	0.301	0.223	0.27	0.27	0.215	0.215	0.59	0.447
$A{\cdot}B$	0.0360	0.39	0.39	0.385	0.3852	9.29	0.005	0.106	0.81	0.81	0.814	0.814	2.25	0.144
$A{\cdot}C$	0.0360	10.25	10.25	10.247	10.2472	247.16	<0.001	0.106	6.56	6.56	6.561	6.561	18.10	<0.001
$A{\cdot}D$	0.0360	3.39	3.39	3.392	3.3921	81.82	<0.001	0.106	4.51	4.51	4.508	4.508	12.43	0.001
$A{\cdot}E$	0.0360	0.67	0.67	0.666	0.6657	16.06	<0.001	0.106	1.31	1.31	1.311	1.311	3.62	0.067
$B{\cdot}C$	0.0360	2.84	2.84	2.838	2.8377	68.45	<0.001	0.106	2.77	2.77	2.771	2.771	7.64	0.010
$B{\cdot}D$	0.0360	0.18	0.18	0.185	0.1845	4.45	0.043	0.106	0.15	0.15	0.147	0.147	0.41	0.529
$B{\cdot}E$	0.0360	1.94	1.94	1.941	1.9407	46.81	<0.001	0.106	4.41	4.41	4.413	4.413	12.17	0.001
$C{\cdot}D$	0.0360	3.78	3.78	3.779	3.7795	91.16	<0.001	0.106	0.023	0.023	0.023	0.023	0.06	0.804
$C{\cdot}E$	0.0360	0.17	0.17	0.169	0.1699	4.10	0.052	0.106	0.045	0.045	0.045	0.045	0.12	0.728
$D{\cdot}E$	0.0360	0.00005	0.00005	0.000	0.0000	0.00	0.973	0.106	0.067	0.067	0.067	0.067	0.19	0.670

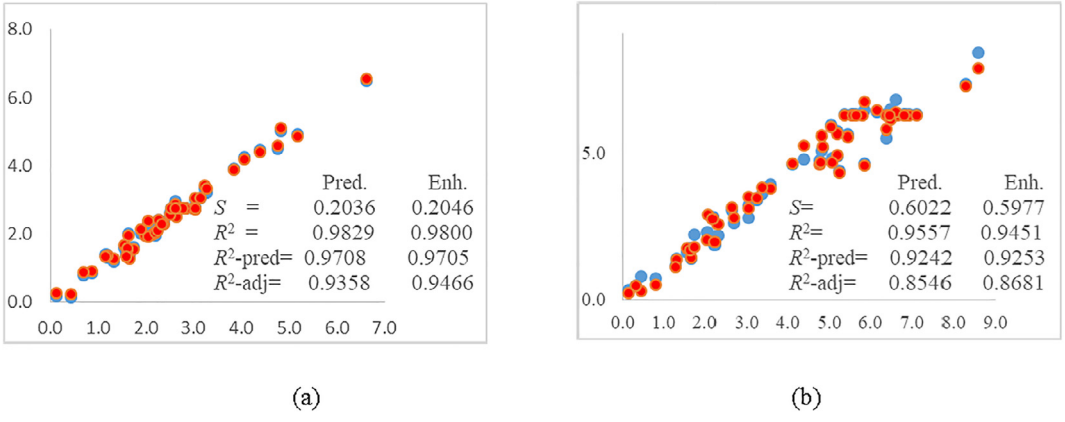

Fig. 4. Regression of experimental values with the calculated values of the predicted and the enhanced models (a) application of agitation speed (200–800 rpm) (b) application of agitation speed (800–1500 rpm).

Table.4
Summary of regression coefficients for full quadratic and enhanced models of protein yields Y_1 (agitation speed 200–800 rpm) and Y_2 (agitation speed 800–1500 rpm).

Regression coefficients	Y_1 models		Y_2 models	
	Full quadratic	Enhanced	Full quadratic	Enhanced
S	0.204	0.205	0.602	0.598
R^2	0.983	0.980	0.956	0.945
R^2_{adj}	0.971	0.971	0.924	0.925
R^2_{pred}	0.936	0.947	0.855	0.868

3.3.2. Enhanced models for protein yields (Y_1) and (Y_2)

The enhanced models were established by deleting the terms with no significant effect ($p > 0.05$) on the extraction process (one -by -one). The enhanced model ($Y_{1(\text{enhanced})}$) composed of 4 linear, 3 quadratic and 8 interactive factors as in (Eq. (8)) while the enhanced model ($Y_{2(\text{enhanced})}$) consisted of 4 linear, 4 quadratic and 5 interactive effects (Eq. (9)).

Table.5
Summary of the analysis of variance (ANOVA) testing the fitness of the regression equations for Y_1 and Y_2.

Source	DF	Y_1 (agitation speed 200–800 rpm)						Y_2 (agitation speed 800–1500 rpm)					
		SS	MS	Adj SS	Adj MS	*F*	*p*	SS	MS	Adj SS	Adj MS	*F*	*p*
Model	22	73.51	73.68	73.971	81.10	0.000	<0.001	220.35	11.02	242.336	11.015	30.38	<0.001
Linear	5			44.500	8.9000	214.67	<0.001			123.204	24.641	67.96	<0.001
Error	31	1.33	0.0429	1.285	0.0415			10.61	0.37	11.241	0.363		
Lack of fit	22	1.23	0.0559	1.102	0.0501	2.46	0.082*	7.76	0.35	7.570	0.344	0.84	0.648*
Pure error	9	0.095	0.0106	0.183	0.0204			2.84	0.41	3.671	0.408		
Total	53	74.84		75.257				230.96		253.576			
Lack of fit for enhanced models				1.324	0.0490	2.41	0.084*			10.260	0.342	0.84	0.665*
Pure error for enhanced models				0.1833	0.0204					3.671	0.408		

* *p* values of *F* were not significant indicating the insignificant lack of fit and accuracy of the models.

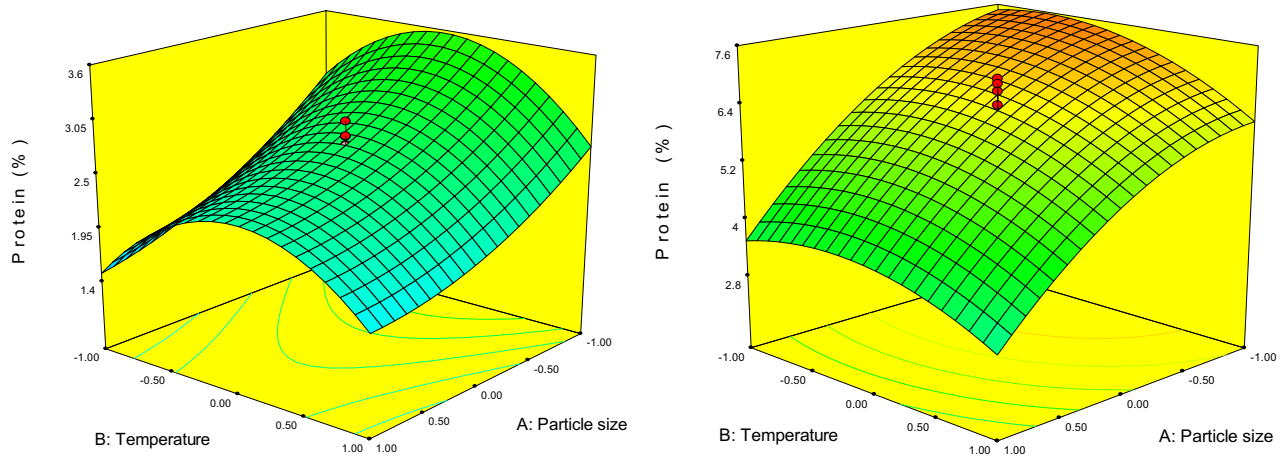

(A) (B)

5.1. Particle size against temperature

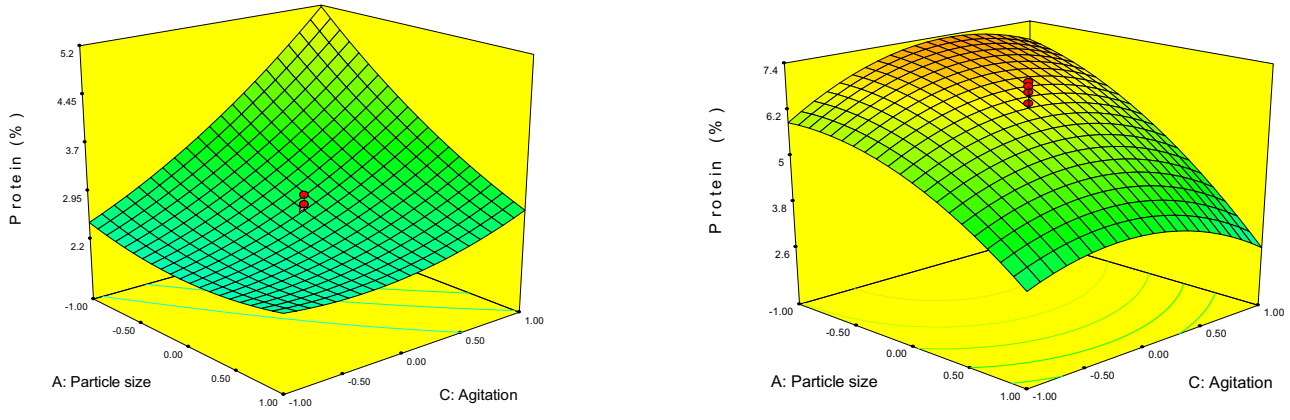

(A) (B)

5.2.Particle size against agitation speed

Fig. 5. 3D surface plots of interactions of the UAE factors. (A) at agitation speed range (200–800 rpm); (B) at agitation speed (800–1500 rpm).

$$Y_{1(\text{enhanced})}\,(\%) = 2.7428 - 0.6002A + 0.7910C + 0.2458D + 0.4553E + 0.1910A^2 - 0.8017B^2 + 0.2277C^2 + 0.1097A \cdot B - 0.5659A \cdot C - 0.3256A \cdot D - 0.1442A \cdot E - 0.2978B \cdot C - 0.0759B \cdot D - 0.2463B \cdot E + 0.3437C \cdot D \quad (8)$$

$$Y_{2(\text{enhanced})}\,(\%) = 6.223 - 1.690A - 0.491B + 0.497D + 0.351E - 0.708A^2 - 0.592B^2 - 0.892C^2 - 0.720D^2 - 0.453A \cdot C - 0.375A \cdot D - 0.294B \cdot C - 0.371B \cdot E \quad (9)$$

3.3.3. Statistical analysis of the models

ANOVA tests were conducted in Minitab 17; the statistical results (Table 3) illustrated significance of the regression coefficients associated with all the terms of the quadratic models. Other results illustrated that the standard errors of regression (S) for predicted and enhanced models were low indicating reasonable variation within the experimental data around the best fit line. The coefficients R^2 and R^2_{adj} illustrated high capabilities of the models to represent the experimental data of the obtained yields. Visualization of experimental values versus the calculated values of the predicted and the enhanced models was in accord with the values of R^2 (Fig. 4). The values of R^2_{pred} slightly increased with the application of the enhanced models indicating higher capability than the quadratic models to predict the mathematical values of the protein yields. The

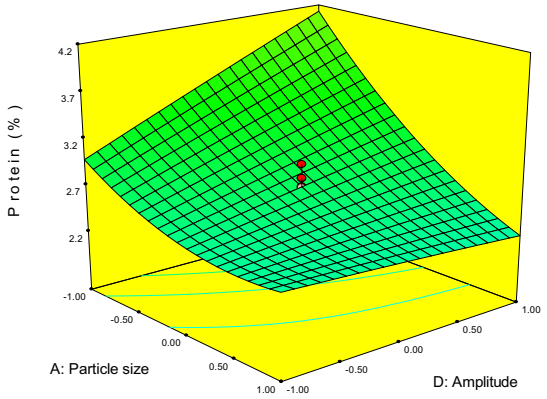

(A)

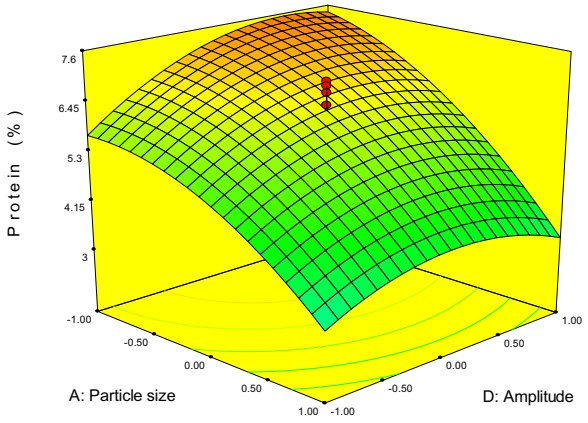

(B)

5.3. Particle size against amplitude

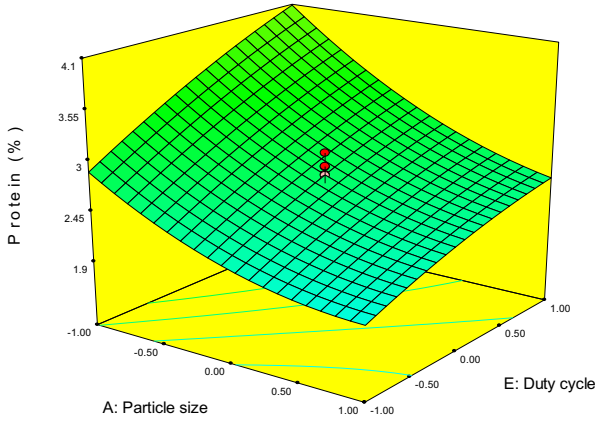

(A)

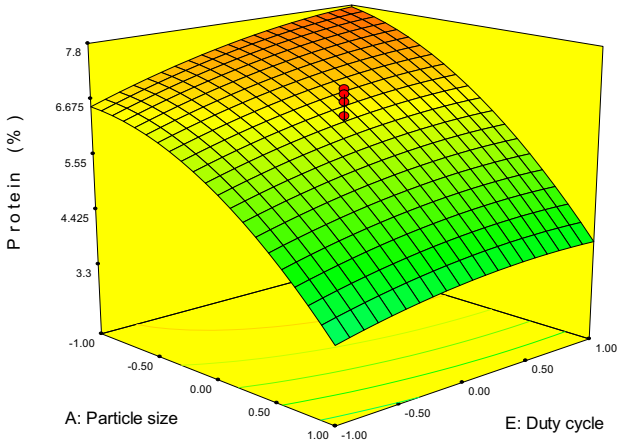

(B)

5.4.Particle size against duty cycle

Fig. 5 (*continued*)

accuracy of the models were also evaluated by the lack of fit test (Table 4); both quadratic and enhanced models revealed adequacy for explaining the models as the p values of lack of fit were insignificant ($p > 0.05$) (See Table 5).

3.4. Surface plots of interactive effects

The 3D plots illustrated that the application of different agitation speeds altered the topographical features of the interactive effects for all the extraction factors (Fig. 5) of Y_1 and Y_2.

Surface plots that investigated the effect of particle sizes (Fig. 5.1–5.4) illustrated a reverse relationship between the particle size and protein yields for Y_1 (Russin et al., 2007) due to the decline in the average diffusion path within the solid and increase in the exchange area between the solid and the solvent. This accelerated the mass transfer (Campbell and Glatz, 2009) and eventually, enhanced the diffusion mechanism (Chan et al., 2014). With the application of higher agitation speeds Y_2 an optimum point of protein yields was detected followed by decrease with the increase of agitation speeds; this decrease may be due to the reduction of solute–solvent collisions in high turbulences (Lebovka et al., 2011) in addition to the impact of the vortex effects (Mohamad et al., 2013).

Determination of a suitable temperature is important to practice a proficient practice of UAE in order to avoid degradation of the bioactive compounds (Meullemiestre et al., 2016). Therefore

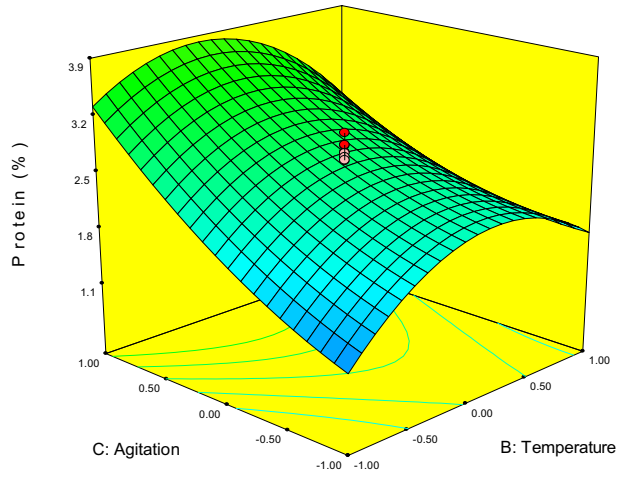

(A)

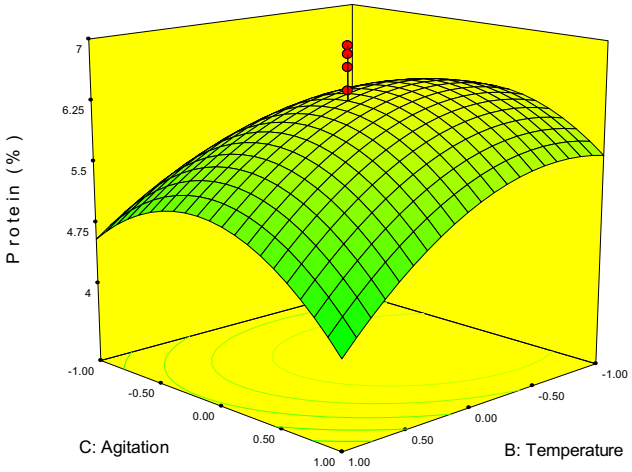

(B)

5.5. Temperature against agitation speed

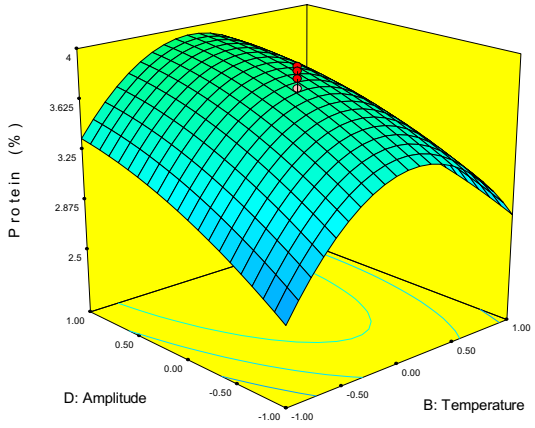

(A)

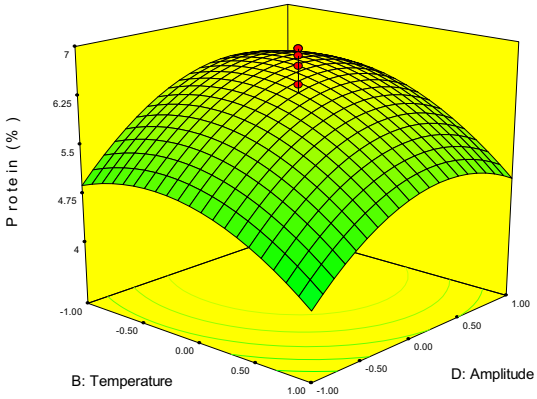

(B)

5.6.Temperature against amplitude

Fig. 5 (*continued*)

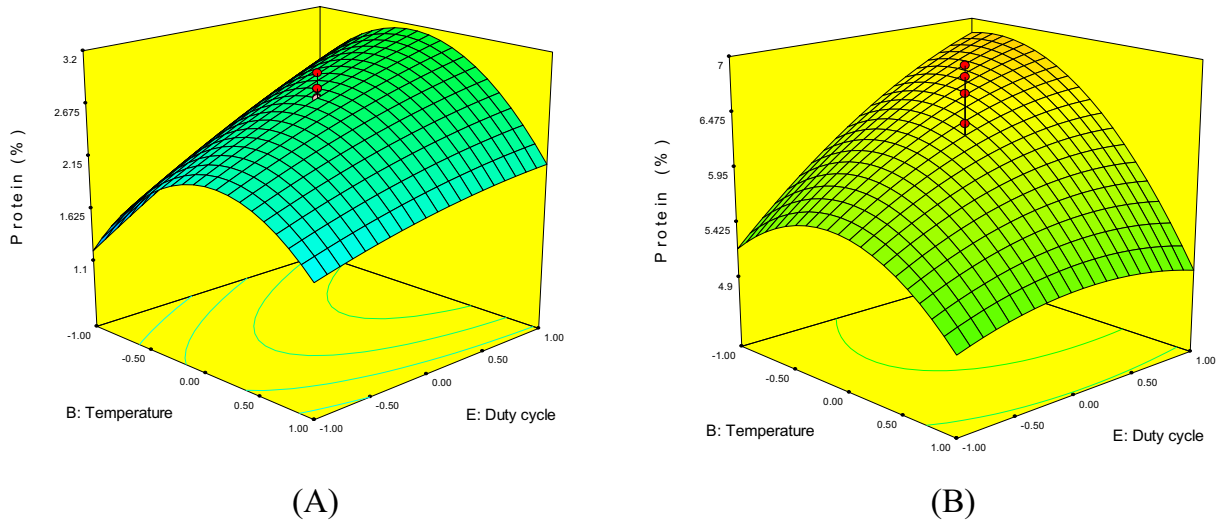

(A) (B)

5.7. Temperature against duty cycle

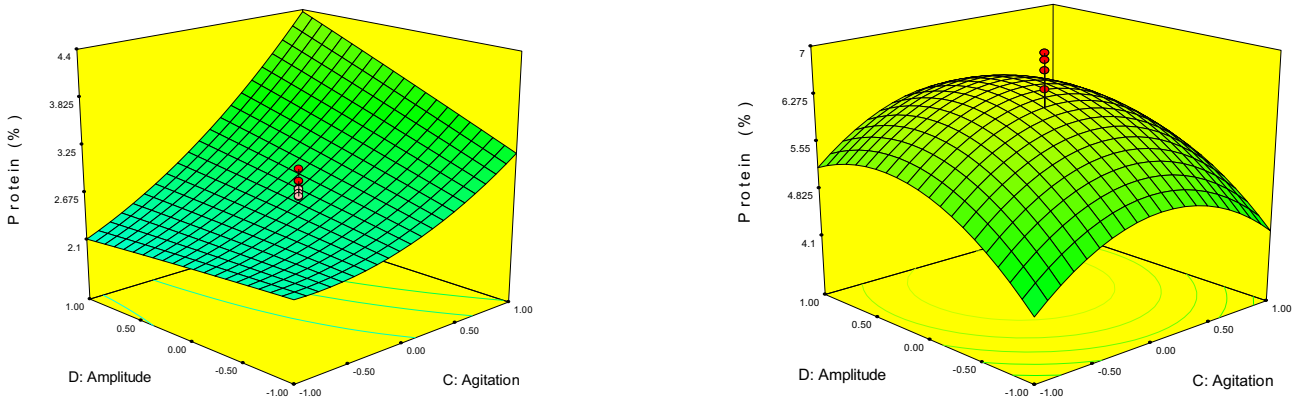

(A) (B)

5.8.Amplitude against agitation

Fig. 5 (*continued*)

temperature was considered as a complex factor in UAE because it was a combination of heat introduced by both the hot plate and ultrasound (Xu and Pan, 2013). Surface plots (5.1, 5.5–5.7) illustrated the quadratic effect of the applied temperature which caused increase in the protein yields until an optimum was reached followed by a decrease in the protein yields as the temperature increased. This reflected the beneficial effect of moderate temperature (Esclapez et al., 2011) for extracting proteins (Barba et al., 2015) while high temperature caused a decrease in the protein yields due to protein denaturation by structural alterations and hydrolysis of peptide bonds of proteins that impact the protein functionality such as solubility (Hojilla-Evangelista and Evangelista, 2009).

Sonication processes were preferred in low temperatures accompanied with a control mechanism to limit temperature rise (Sališová et al., 1997) which was inevitable during sonication (Tiwari, 2015). However, in this study, the mechanical agitation seemed to work as a cooling factor (Taraba et al., 2012), especially at high agitation speeds. Low temperatures induced lower vapor pressure that allowed stronger collapses of the cavitation bubbles (Tiwari, 2015) while high temperatures resulted in increasing the vapor pressure that could have caused the filling of the voids with water resulting in gentle collapses of the cavitation bubbles (Santos et al., 2009).

The study illustrated the importance of determining a suitable agitation speed to provide a suitable extraction environment for all the combined factors. Surface plots (Fig. 5.2, 5.5, 5.8 and 5.9) demonstrated a proportional relationship between the protein yields and the increasing agitation speed until the optimum yields were obtained, followed by a decrease in protein yields due to that extreme agitation speed formations (Mohamad et al., 2013).

Ultrasound was introduced by a probe tip dipped 30 mm at the center of the solvent surface for maximum effect. Surface plots (5.2, 5.3 5.6–5.10) illustrated the interactive effects of the ultrasound regiments, amplitude and duty cycle (%), with the other extraction factors. Application of ultrasound with suitable pulse pause operations (duty cycle %) are more efficient than continuous sonication (Xu and Pan, 2013) and provided better sonication

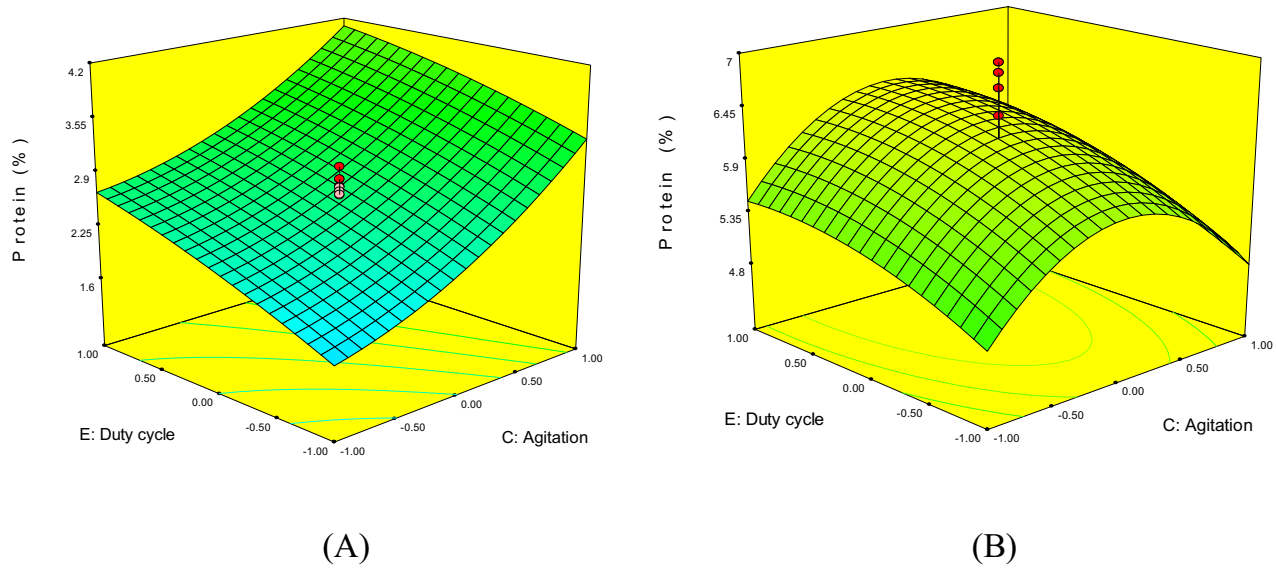

(A) (B)

5.9. Duty cycle against agitation speed

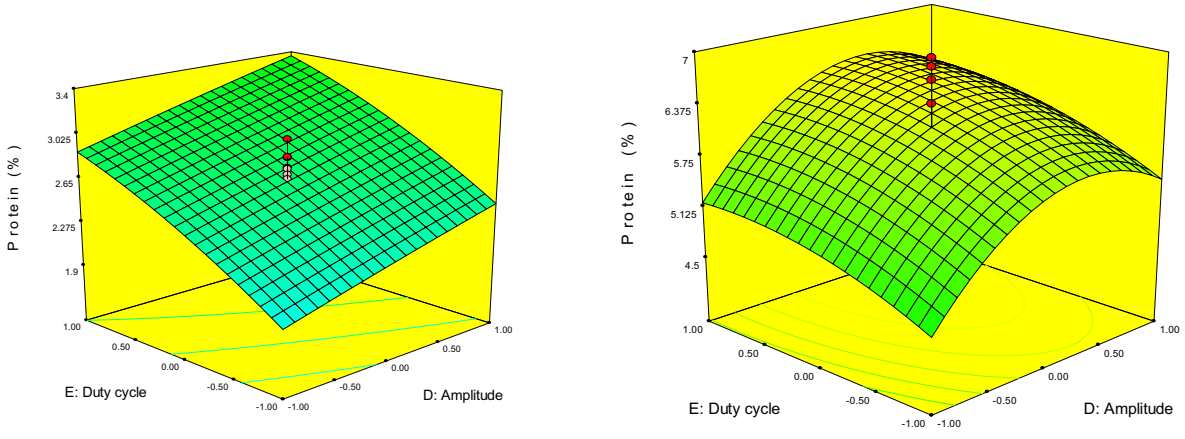

(A) (B)

5.10.Amplitude against duty cycle

Fig. 5 (*continued*)

performance (Mitome and Hatanaka, 2002). Low ultrasound intensities were considered because they are non-destructive for natural constituents (Raso et al., 1999). The effects of amplitude and duty cycle revealed a proportional effect of increasing amplitude at low agitation speeds; that altered to a quadratic effect at higher agitation speeds. This implied that there was a negative effect of excessive turbulences that could have impacted the dissipation of cavitation bubbles in the solvent and reduced their impacts on the solid particles.

In this study, sonication time was fixed to 5 min to avoid ultrasound degradation by exceeding sonication time (Xu and Pan, 2013), application of high frequencies (Achat et al., 2012) or by thermal impacts (Jacotet-Navarro et al., 2016) and the application of sonication in initiating extraction processes to facilitate the metabolite extraction (Seidel, 2012). However protein degradation could have occurred due to other factors in the sonication process such as the high intensity of ultrasound at the probe tip (Veillet et al., 2010) or the increase of the enthalpy of denaturation by the aggregation phenomena (Chandrapala et al., 2011).

3.5. Ultrasound intensity (UI)

To avoid the misleading of evaluating the ultrasound power efficiency only by the amplitude and duty cycle, the ultrasonic intensity (UI) was estimated in each experiment as in (Eq. (3)) (Boukroufa et al., 2015; Pingret et al., 2012) by employing the calculated sonication power in (Eq. (2)) and the change of solvent temperature through the sonication time (Carail et al., 2015; Sicaire et al., 2016). With the application of low agitation speeds (200–800 rpm), *UI* ranged between 0.02 and 2.95 $W{\cdot}cm^{-2}$ and at

high agitation speed (800–1500 rpm) from 1.06 to 5.1 W·cm^{-2} (Table 2).

The effects of the extraction factors; temperature, agitation speed, amplitude and duty cycle on the ultrasonic intensity were studied and visualized (Figs. 6 and 7). Surface plots (Fig. 6) illustrated the interactive effects of these factors on the *UI* values with the application of agitation speed range (200–800 rpm). *UI* increased with the decrease of temperature and the increase of agitation speed. This might be due to the low vapor pressure at low temperatures that assured the violent collapse of the cavitation bubbles. The *UI* increased with the increase of both the amplitude and duty cycle until an optimum point was reached followed by a decrease in the intensification; this might be explained by that high amplitudes and excessive pulse durations caused the increase of the temperature which caused gentle collapses of the cavitation bubbles that attenuate the ultrasound efficiency (Santos et al., 2009).

Surface plots (Fig. 7) illustrated alterations in the interactive effects of the extraction factors with the application of agitation speed range (800–1500 rpm) except for temperature. *UI* decreased with the increase of agitation speed that implied the negative impact of high turbulences. The increase of the amplitude caused

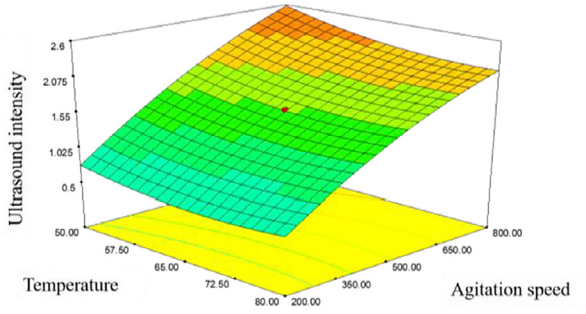

Fig.6.1. Temperature against agitation speed

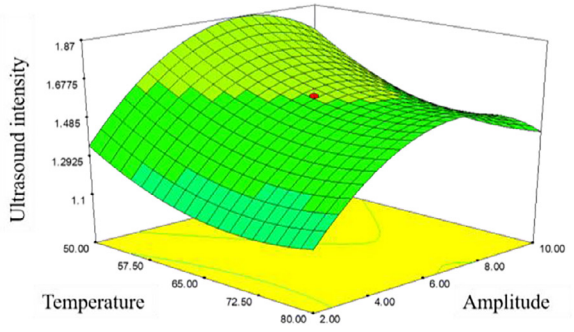

Fig. 6.2. Temperature against Amplitude

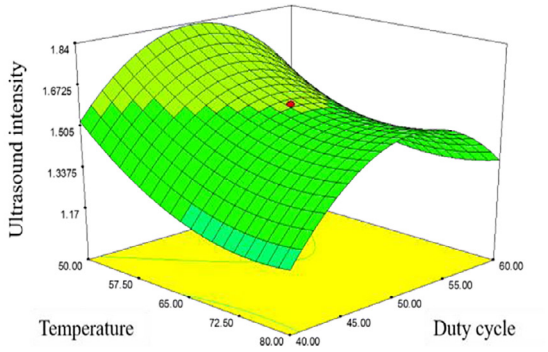

Fig. 6.3. Temperature against duty cycle

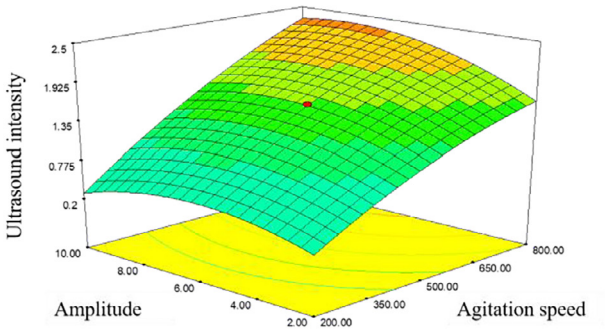

Fig.6.4. Amplitude against agitation speed

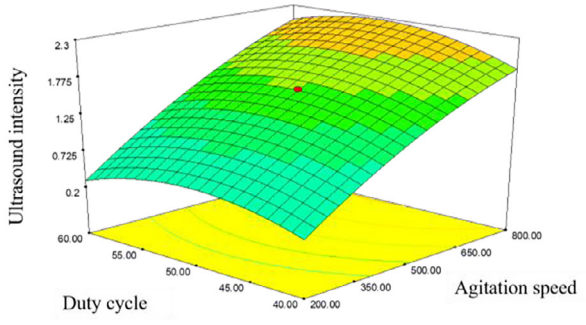

Fig. 6.5. Agitation speed against duty cycle

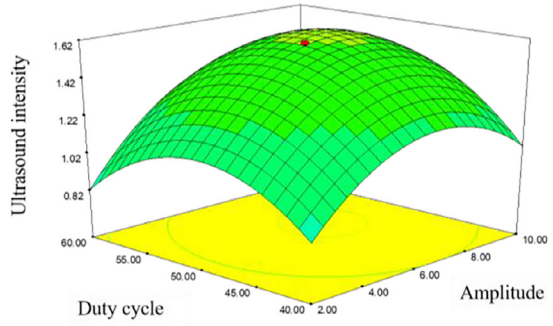

Fig. 6.6. Amplitude against duty cycle

Fig. 6. Interactive effects of sonication factors on the ultrasound intensity (UI) with the application of agitation speed (200–800 rpm).

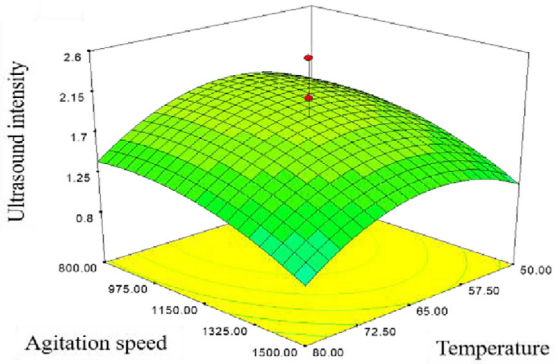

Fig.7.1. Temperature against agitation speed

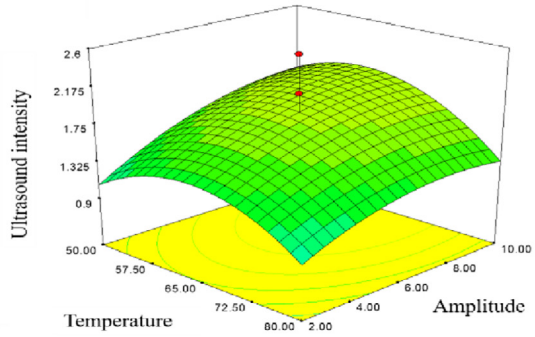

Fig. 7.2. Temperature against Amplitude

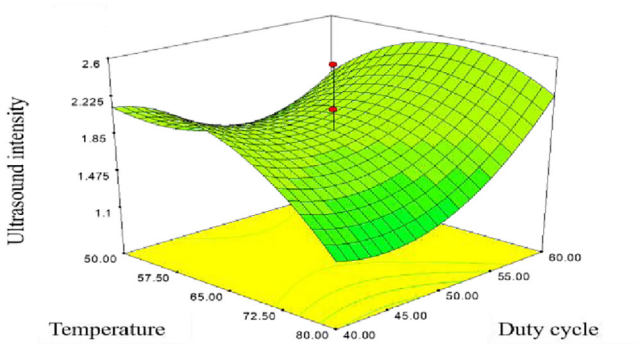

Fig. 7.3. Temperature against duty cycle

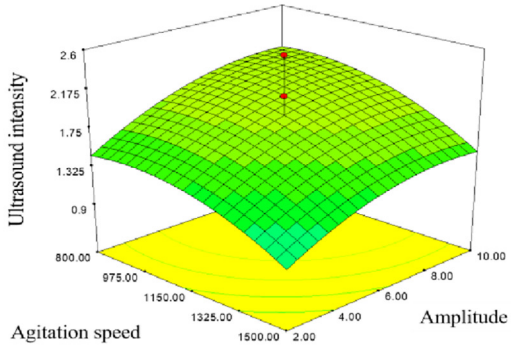

Fig.7.4. Amplitude against agitation speed

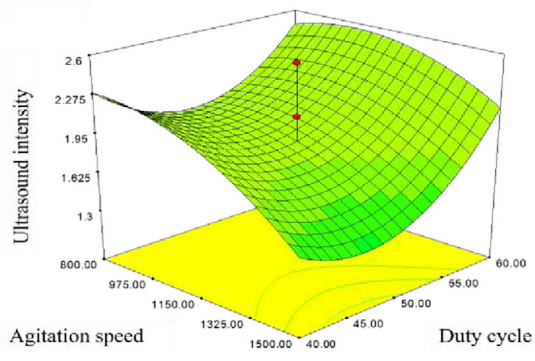

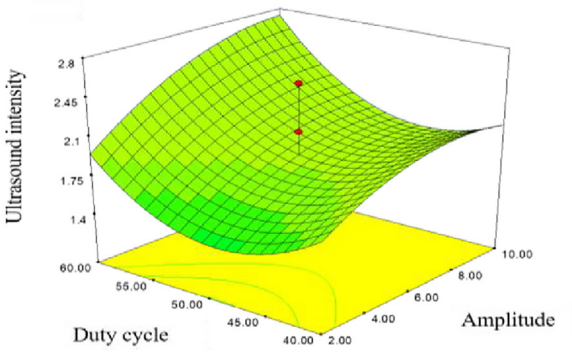

Fig. 7. Interactive effects of sonication factors on the ultrasound intensity (UI) with the application of agitation speed (800–1500 rpm).

an increase in *UI* until the optimum was reached and followed by a decrease. The increase of the duty cycle caused an increase in the *UI* which allowed more ultrasound energy to be dissipated as heat in the extraction system.

Further investigation employed CCCD models for the particle size, temperature and agitation speed ranges and *UI* instead of amplitude and duty cycle. Statistical results (Table 6) demonstrated the accuracy of the models by the high values of the R^2, R^2_{adj} and R^2_{pred} for both the quadratic models (Eqs. (10) and (11)) and the enhanced models (Eqs. (12) and (13)). The increase in R^2_{pred} values of the enhanced models illustrated higher capacity of predicting the protein yields (Y_1 and Y_2).

$$Y_{1(quadratic)} = 2.58 - 0.71A + 0.063B + 1.00C + 0.62UD + 0.29A^2 - 0.99B^2 - 0.39C^2 + 1.52UI^2 - 0.034A \cdot B - 0.074A \cdot C - 0.92A \cdot UI - 0.048B \cdot C - 0.088B \cdot UI + 0.70C \cdot UI \quad (10)$$

$$Y_{2(quadratic)} = 6.90 - 2.44A - 0.69B - 0.46C + 1.89UI - 0.96A^2 - 0.48B^2 - 1.16C^2 - 0.38UI^2 - 0.063A \cdot B - 0.34A \cdot C - 1.54A \cdot UI - 0.24B \cdot C - 0.80B \cdot UI - 0.69C \cdot UI \quad (11)$$

Table 6
ANOVA for protein yields (%) Y_1 and Y_2 based on the effect of ultrasonic intensity (*UI*).

Source		Df	Y_1: agitation speed range (200–800 rpm)				Y_2: agitation speed range (800–1500 rpm)			
			SS	MS	*F*- ratio	*p*-value	SS	MS	*F*-ratio	*p*-value
A: particle size (radius = mm)		1	9.61	9.61	114.57	<0.05	47.50	47.50	124.91	<0.05
B: Temperature (°C)		1	0.077	0.077	0.92	**0.3432**	3.15	3.15	8.27	<0.05
C: Agitation speed (rpm)		1	7.56	7.56	90.08	<0.05	1.18	1.18	3.09	**0.0874**
UI: ultrasonic intensity		1	1.49	1.49	17.76	<0.05	4.44	4.44	11.67	<0.05
A·B		1	0.034	0.034	0.40	**0.5309**	0.11	0.11	0.28	**0.5981**
A·C		1	0.047	0.047	0.56	**0.4582**	3.67	3.67	9.66	<0.05
A·UI		1	2.80	2.80	33.41	<0.05	6.49	6.49	17.07	<0.05
B·C		1	0.017	0.017	0.20	**0.6545**	1.45	1.45	3.81	**0.0591**
B·UI		1	0.021	0.021	0.25	**0.6180**	1.41	1.41	3.72	**0.0621**
C·UI		1	0.68	0.68	8.05	<0.05	0.99	0.99	2.61	**0.1151**
A^2		1	0.30	0.30	3.55	**0.0679**	6.56	6.56	17.25	<0.05
B^2		1	6.64	6.64	79.11	<0.05	1.63	1.63	4.28	<0.05
C^2		1	0.48	0.48	5.69	<0.05	7.32	7.32	19.25	<0.05
UI^2		1	1.96	1.96	23.37	<0.05	0.18	0.18	0.47	**0.4959**
residual		37	2.94	0.084			13.31	0.38		
Total (corr.)		53	71.08				247.99			
Quadratic model	R^2		0.959				0.946			
	R^2_{adj}		0.942				0.925			
	R^2_{pred}		0.897				0.854			
Enhanced model	R^2		0.944				0.921			
	R^2_{adj}		0.933				0.906			
	R^2_{pred}		0.909				0.864			

$$Y_{1(enhanced)} = 2.61 - 0.70A + 1.41C + 0.48UI - 0.90B^2 - 0.38C^2 + 1.90UI^2 - 0.98A \cdot UI + 0.60C \cdot UI \quad (12)$$

$$Y_{2(enhanced)} = 6.75 - 2.43A - 0.31B + 1.59UI - 0.80A^2 - 0.49B^2 - 1.41C^2 - 0.37A \cdot C - 1.52A \cdot UI \quad (13)$$

Surface plots (Fig. 8) illustrated the interactive effects of *UI* with the other extraction factors on the protein yields for both agitation speed ranges. With the application of agitation speed range (200–800 rpm) the protein yield initially decreased with the increase of *UI* followed by an increase. The application of high agitation speed range maximized the effect of *UI* with other factor which contributed to the increase of protein yields. The effect of *UI* may be related to the overall temperature of the extraction system and the competence of high agitation speeds to cool down the temperature and dissipate the bubbles more efficiently than low agitation speeds.

3.6. SEM analysis

Structural changes in the samples were visualized by SEM images (Fig. 7) using a Hitachi-TM3030 tabletop microscope. The surface characteristics of *E. longifolia* powder were captured before and after sonication. The surface of the untreated powder were relatively smooth (Fig. 9.a). Root powder treated with ultrasound illustrated morphological alterations after UAE (Fig. 9.b and .c). The images suggested two possible mechanisms that effected the raw material surface; the first was erosion depending of the morphological damage on the surface of the raw material and the second was sonoporation which was implied from the numerous pores in certain parts on the surface (Fig. 9.b). The surface was observed with higher magnification (Fig. 9.c) that showed clearly what the two suggested mechanisms, sonoporation and erosion. Ultrasound effect could be a combination of more than one mechanism that is impacted by the nature of the raw material (Chemat et al., 2017b). However, these findings suggested that the inner structure of the raw material could be impacted with different degrees of various mechanisms. This suggested further investigation on the impact of ultrasound on tissue level. The combination of these mechanisms seemed to cause the ultrasound enhancement of extraction rate by enhancing water accessibility (Chemat et al., 2017b) causing hydration followed by swelling and softening of the plant tissue (Pingret et al., 2013; Toma et al., 2001; Vinatoru, 2001) which improved solubilization (Chemat et al., 2017b).

3.7. Experimental validation of the optimized conditions for the proteins yields and comparison with conventional extraction

Taking in account the significant factors and interactions, the corresponding enhanced models to both sets were used to estimate the extraction times. Conditions for maximizing the yield was estimated by the maximum desirability in Minitab 17. The predicted maximizing conditions for Y_1 were *A*: 0.022 ± 0.022 mm, *B*: 56 °C, *C*: 897 rpm, *D*: 11 W and *E*: 63% with a *UI*: 2.26 W·cm^{-2} and predicted maximum yield of 8.5102% while for Y_2 were *A*: 0.022 ± 0.022 mm, *B*: 49 °C, *C*: 1314 rpm, *D*: 9 W and *E*: 63% with a *UI*: 2.94 W·cm^{-2} and predicted maximum yield of 9.2317% after 5 min of sonication.

Experimental results of the protein yield for $Y_{1(enhanced)}$ was 8.341 ± 0.371% while for $Y_{2(enhanced)}$ it was 9.543 ± 0. 946% ($N = 5$) after extraction for 5 min. Both results showed no significant differences ($p < 0.05$) which proved the validity of the designed model in this study. The significant of this study was demonstrated by a comparison by applying the optimum conditions of the UAE with the conventional heat assisted extraction (HAE) process. The conventional process conditions included all the factors of UAE except amplitude and duty cycle (%). The nearest yield value was between 36 min (9.471 ± 0.149%) and 38 min (9.761 ± 0.728) which was nearly 7 times the UAE extraction duration (Fig. 10). The results proved the efficiency of UAE to decrease the extraction time. UAE is known to improve the extraction process with noticeable reduction of extraction time (Da Porto et al., 2013) for proteins (Preece et al., 2016), which ultimately provides less time and energy (Chemat and Khan, 2011). The yield of the extracted protein by UAE was approximately 60% of the total water extractable proteins (9% out of 15% of total protein). This amount of proteins was obtained after a short extraction duration (5 min), therefore,

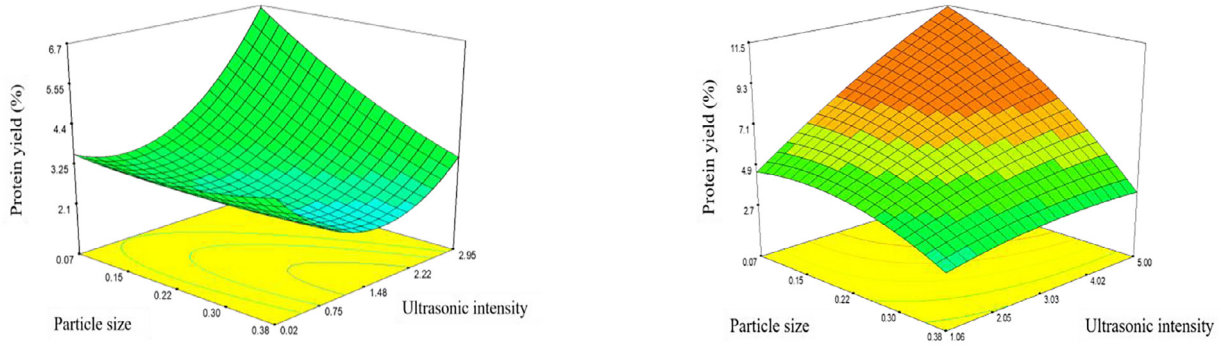

(a) (b)

8.a. Interactive effects of UI and particle size on the protein yield.

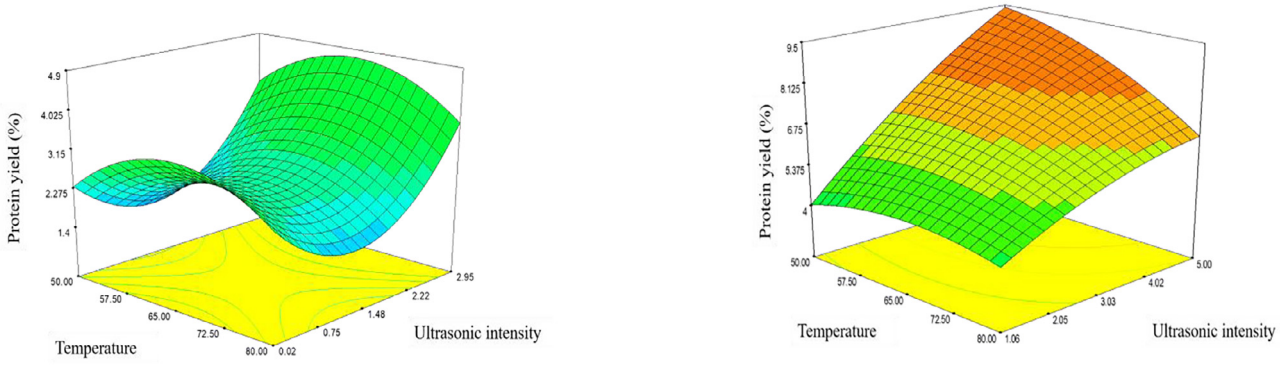

(a) (b)

8.b. Interactive effects of UI and temperature on the protein yield.

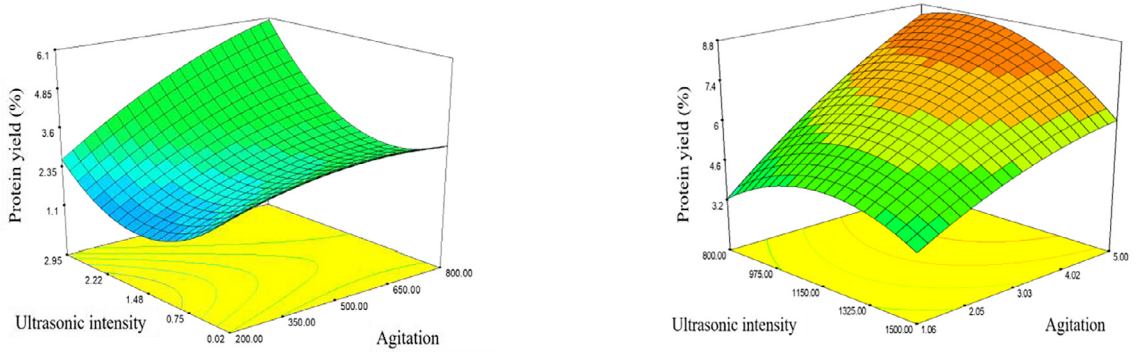

(a) (b)

8.c. Interactive effects of UI and agitation speed size on the protein yield.

Fig. 8. Interactive effects of UI with other extraction factors on the protein yields (%). (a) Agitation speed range (200–800 rpm); (b) Agitation speed range (800–1500 rpm).

suitable modifications could be applied such as increasing extraction time to obtain more proteins.

3.8. Upscaling and industrialization applications

Industrial production of *E. longifolia* root extracts is highly demanded due to the massive consumption of commercial *E. longifolia* root products (Vejayan et al., 2013). The upscaling of eurycomanone yield (3%) from laboratory findings to pilot and industrial scales have been experimented without regard to the thermosliable metabolites, at 100 °C and above, either by experiments or stimulations (Abdul-Aziz et al., 2014; Athimulam et al., 2006). However, this condition (100 °C and above) was known to cause denaturation of the proteins (Kinsella, 1979). The rising of the herbal – based phytochemical industry in Malaysia necessitate solutions to the drawbacks associated with this industrial sector to produce medicinal and food supplements with high quality. Products of *E. longifolia* are highly demanded in this herbal market which required the implementation of green extraction techniques instead of the conventional techniques, such as UAE, that could

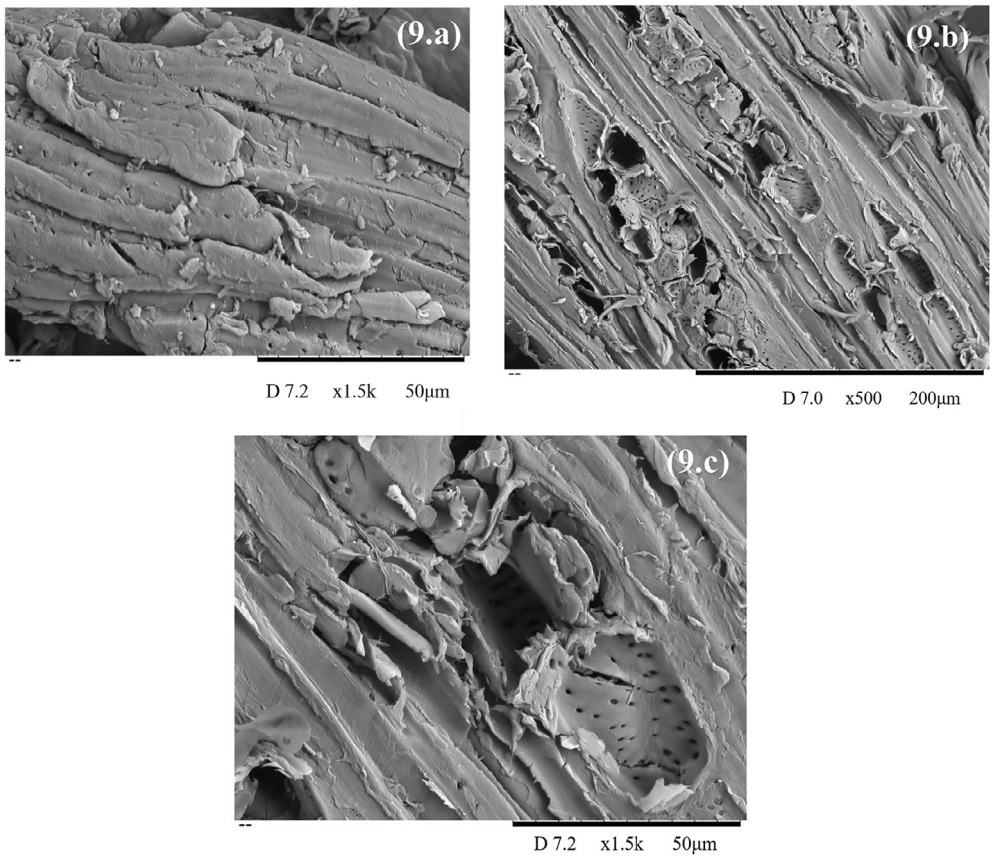

Fig. 9. SEM images of Eurycoma longifolia roots (pulverized), (9.a) Dry root before ultrasonic treatment (×1.5 k), (9.b) Root after ultrasonic treatment (×500) and (9.c) Root after ultrasonic treatment (1.5 k).

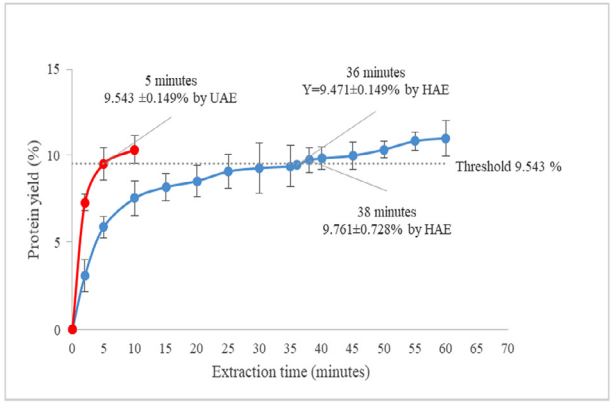

Fig. 10. Comparison between UAE and HAE with a determined threshold of 9.543% protein yield.

contribute to enhancing the yield, lowering the temperature and operating costs at short extraction durations (Achat et al., 2012; Boukroufa et al., 2015) in addition to other aspects such as protection of the consumer and the environment and enhancement of innovative industry practice (Chemat et al., 2012; Rombaut et al., 2014). This study introduced an alternative and a promising method to extract proteins at optimum conditions that could be used to upscale the protein extraction process to pilot and industrial scales (Chemat et al., 2017a) which require industrial setups with larger solvent volumes and higher ultrasound powers (Chemat et al., 2017b).

4. Conclusions

This study illustrated for the first time optimization process of extracting proteins from *E. longifolia* roots by UAE. The results showed that the effect of agitation speeds on the efficiency of the extraction process with the other four factors. The results also suggested that the extraction process was actually a combination of two criteria. The first was due to the agitation effect on the conventional factors. The variety in agitation speed affect the diffusion of the solutes from the particles and cooling the extraction temperature at high stirring velocities. From the two experimental sets, the parameters of the second enhanced model (Y_2) prevailed to be more efficient in protein recovery with optimum conditions of *A*: 0.022 ± 0.022 mm, *B*: 49 °C, *C*: 1314 rpm, *D*: 9 W, *E*: 63% and *UI*: 2.94 W.cm^{-2} was 9.543 ± 0. 946%. High agitation speed didn't only affect the solvent properties, the diffusion of the solutes from the particles, cooling the extraction temperature, but influenced the distribution of cavitation bubbles and their impact on the solid particles. This implied that the extraction procedure was actually a dual extraction process of conventional and nonconventional method combined together. The study was compared with a conventional extraction process that employed the optimum conditions except the sonication. The UAE reduced the conventional extraction duration that reached approximately the same yield concentration of UAE around 7 times.

Acknowledgements

We gratefully acknowledge the Ministry of Agriculture (MOA), Malaysia, for the financial support under the grants (RDU 161601); Ministry of Higher Education, (MOHE), Malaysia (RDU

160801) and Universiti Malaysia Pahang (UMP) Doctoral Scheme Scholarship (DSS).

References

Abdul-Aziz, A., Yaakob, H., Aziz, R., Rahman, R.A., Ngadiran, S., Muhammad, M.F., Harun, N.H., Zamri, W.M.W., Rosly, E.S., 2014. Case study: statistical analysis of eurycomanone yield using a full factorial design. In: Granato, D. (Ed.), Mathematical and Statistical Methods in Food Science and Technology. John Wiley and Sons, Chichester, UK, pp. 43–54.

Abugabr Elhag, H.E.E., Sulaiman, A.Z., Ajit, A., 2016. A review on the extraction methods of extracts and phytochemicals from Eurycoma longifolia (Tongkat Ali Jack). In: National Conference for Postgraduate Research (NCON-PGR 2016). Universiti Malaysia Pahang, Pekan. Session 1. 32. 24–25th September 2016.

Achat, S., Tomao, V., Madani, K., Chibane, M., Elmaataoui, M., Dangles, O., Chemat, F., 2012. Direct enrichment of olive oil in oleuropein by ultrasound-assisted maceration at laboratory and pilot plant scale. Ultrason. Sonochem. 19, 777–786.

Aguiló-Aguayo, I., Walton, J., Viñas, I., Tiwari, B.K., 2017. Ultrasound assisted extraction of polysaccharides from mushroom by-products. LWT – Food Sci. Technol. 77, 92–99.

Alvarez, M.M., Arratia, P.E., Muzzio, F.J., 2002. Laminar mixing in eccentric stirred tank systems. Can. J. Chem. Eng. 80, 546–557.

Athimulam, A., Kumaresan, S., Foo, D.C.Y., Sarmidi, M.R., Aziz, R., 2006. Modelling and optimization of *Eurycoma longifolia* water extract production. Food Bioprod. Process. 84, 139–149.

Barba, F.J., Galanakis, C.M., Esteve, M.J., Frigola, A., Vorobiev, E., 2015. Potential use of pulsed electric technologies and ultrasounds to improve the recovery of high-added value compounds from blackberries. J. Food Eng. 167, 38–44.

Boukroufa, M., Boutekedjiret, C., Petigny, L., Rakotomanomana, N., Chemat, F., 2015. Bio-refinery of orange peels waste: a new concept based on integrated green and solvent free extraction processes using ultrasound and microwave techniques to obtain essential oil, polyphenols and pectin. Ultrason. Sonochem. 24, 72–79.

Caleja, C., Barros, L., Prieto, M., Barreiro, M.F., Oliveira, M.B.P., Ferreira, I.C., 2017. Extraction of rosmarinic acid from *Melissa officinalis* L. by heat-, microwave-and ultrasound-assisted extraction techniques: a comparative study through response surface analysis. Sep. Purif. Technol. 186, 297–308.

Campbell, K., Glatz, C.E., 2009. Mechanisms of aqueous extraction of soybean oil. J. Agric. Food Chem. 57, 10904–10912.

Carail, M., Fabiano-Tixier, A.S., Meullemiestre, A., Chemat, F., Caris-Veyrat, C., 2015. Effects of high power ultrasound on all-E-beta-carotene, newly formed compounds analysis by ultra-high-performance liquid chromatography-tandem mass spectrometry. Ultrason. Sonochem. 26, 200–209.

Chan, C.H., Yusoff, R., Ngoh, G.-C., 2014. Modeling and kinetics study of conventional and assisted batch solvent extraction. Chem. Eng. Res. Des. 92, 1169–1186.

Chandrapala, J., Zisu, B., Palmer, M., Kentish, S., Ashokkumar, M., 2011. Effects of ultrasound on the thermal and structural characteristics of proteins in reconstituted whey protein concentrate. Ultrason. Sonochem. 18, 951–957.

Chemat, F., Khan, M.K., 2011. Applications of ultrasound in food technology: processing, preservation and extraction. Ultrason. Sonochem. 18, 813–835.

Chemat, F., Rombaut, N., Meullemiestre, A., Turk, M., Perino, S., Fabiano-Tixier, A.-S., Abert-Vian, M., 2017a. Review of green food processing techniques. Preservation, transformation, and extraction. Innov. Food Sci. Emerg. Technol. 41, 357–377.

Chemat, F., Rombaut, N., Sicaire, A.-G., Meullemiestre, A., Fabiano-Tixier, A.-S., Abert-Vian, M., 2017b. Ultrasound assisted extraction of food and natural products. mechanisms, techniques, combinations, protocols and applications. A review. Ultrason. Sonochem. 34, 540–560.

Chemat, F., Vian, M.A., Cravotto, G., 2012. Green extraction of natural products: concept and principles. Int. J. Mol. Sci. 13, 8615–8627.

Chua, L.S., Abd Rahman, N., Sarmidi, M.R., 2014. Plant protein extraction and identification from *Eurycoma longifolia* by gel electrophoresis and mass spectrometry. Curr. Proteomics 11, 161–170.

Chua, L.S., Abdul-Rahman, N., Rosidi, B., Lee, C.T., 2013. Plant proteins, minerals and trace elements of *Eurycoma longifolia* (Tongkat Ali). Nat. Prod. Res. 27, 314–318.

Da Porto, C., Porretto, E., Decorti, D., 2013. Comparison of ultrasound-assisted extraction with conventional extraction methods of oil and polyphenols from grape (*Vitis vinifera* L.) seeds. Ultrason. Sonochem. 20, 1076–1080.

Danial, M., Saghal, G., Mubbarakh, S.A., Sundarasekar, J., Subramaniam, S., 2013. Antibacterial studies on in vivo plant parts of medicinally important *Eurycoma longifolia* (Tongkat Ali). Pak. J. Bot. 45, 1693–1700.

Esclapez, M., García-Pérez, J., Mulet, A., Cárcel, J., 2011. Ultrasound-assisted extraction of natural products. Food. Eng. Rev. 3, 108–120.

Fang, G., Li, G., Pang, C., Li, W., Wang, D., Liu, C., 2016. Ultrasound-assisted extraction of pristimerin from *Celastrus orbiculatus* using response surface methodology. Biol. Pharm. Bull.

Ghitescu, R.-E., Volf, I., Carausu, C., Bühlmann, A.-M., Gilca, I.A., Popa, V.I., 2015. Optimization of ultrasound-assisted extraction of polyphenols from spruce wood bark. Ultrason. Sonochem. 22, 535–541.

Harun, N.H., Abdul-Aziz, A., Aziz, R., 2015. Effect of number of steps on the quality of *Eurycoma longifolia* extract and cost efficiency of the extraction process. Trans. Sci. Technol. 2, 36–47.

Higuera-Barraza, O., Torres-Arreola, W., Ezquerra-Brauer, J., Cinco-Moroyoqui, F., Figueroa, J.R., Marquez-Ríos, E., 2017. Effect of pulsed ultrasound on the physicochemical characteristics and emulsifying properties of squid (*Dosidicus gigas*) mantle proteins. Ultrason. Sonochem. 38, 829–834.

Hojilla-Evangelista, M.P., Evangelista, R.L., 2009. Functional properties of protein from *Lesquerella fendleri* seed and press cake from oil processing. Ind. Crop. Prod. 29, 466–472.

Jacotet-Navarro, M., Rombaut, N., Deslis, S., Fabiano-Tixier, A.S., Pierre, F.X., Bily, A., Chemat, F., 2016. Towards a "dry" bio-refinery without solvents or added water using microwaves and ultrasound for total valorization of fruit and vegetable by-products. Green Chem. 18, 3106–3115.

Jiang, S., Ding, J., Andrade, J., Rababah, T.M., Almajwal, A., Abulmeaty, M.M., Feng, H., 2017. Modifying the physicochemical properties of pea protein by pH-shifting and ultrasound combined treatments. Ultrason. Sonochem. 38, 835–842.

Kadam, S.U., Tiwari, B.K., Álvarez, C., O'Donnell, C.P., 2015. Ultrasound applications for the extraction, identification and delivery of food proteins and bioactive peptides. Trends Food Sci. Technol. 46, 60–67.

Khanam, Z., Wen, C.S., Bhat, I.U.H., 2015. Phytochemical screening and antimicrobial activity of root and stem extracts of wild *Eurycoma longifolia* Jack (Tongkat Ali). J. King Saud Univ. Sci. 27, 23–30.

Kinsella, J.E., 1979. Functional properties of soy proteins. J. Am. Oil Chem. Soc. 56, 242–258.

Kumari, B., Tiwari, B.K., Hossain, M.B., Rai, D.K., Brunton, N.P., 2017. Ultrasound-assisted extraction of polyphenols from potato peels: profiling and kinetic modelling. Int. J. Food Sci. Technol. 52, 1432–1439.

Lebovka, N., Vorobiev, E., Chemat, F., 2011. Enhancing Extraction Processes in the Food Industry. CRC Press.

Leonelli, C., Mason, T.J., 2010. Microwave and ultrasonic processing: now a realistic option for industry. Chem. Eng. Process. Process Intensif. 49, 885–900.

Li, S., Ma, H., Guo, Y., Oladejo, A.O., Yang, X., Liang, Q., Duan, Y., 2018. A new kinetic model of ultrasound-assisted pretreatment on rice protein. Ultrason. Sonochem. 40, 644–650.

Low, W.-Y., Tan, H.-M., 2007. Asian traditional medicine for erectile dysfunction. J. Men's Health Gender 4, 245–250.

Lowry, O.H., Rosebrough, N.J., Farr, A.L., Randall, R.J., 1951. Protein measurement with the Folin phenol reagent. J. Biol. Chem. 193, 265–275.

Lupatini, A.L., de Oliveira Bispo, L., Colla, L.M., Costa, J.A.V., Canan, C., Colla, E., 2016. Protein and carbohydrate extraction from *S. platensis* biomass by ultrasound and mechanical agitation. Food Res. Int.

Malaysian Standard, 2011 Pages 12. In: Phytopharmaceutical Aspects of Freeze Dried Water Extract from Tongkat Ali Roots-Specification. Jabatan Standard Malaysia, USA, pp. 1–13.

Malik, M.A., Sharma, H.K., Saini, C.S., 2017. High intensity ultrasound treatment of protein isolate extracted from dephenolized sunflower meal: effect on physicochemical and functional properties. Ultrason. Sonochem.

Mane, S., Bremner, D.H., Tziboula-Clarke, A., Lemos, M.A., 2015. Effect of ultrasound on the extraction of total anthocyanins from Purple Majesty potato. Ultrason. Sonochem. 27, 509–514.

Meullemiestre, A., Petitcolas, E., Maache-Rezzoug, Z., Chemat, F., Rezzoug, S.A., 2016. Impact of ultrasound on solid–liquid extraction of phenolic compounds from maritime pine sawdust waste. Kinetics, optimization and large scale experiments. Ultrason. Sonochem. 28, 230–239.

Minitab, I., 2014. MINITAB release 17: Statistical Software for Windows. Minitab Inc, USA.

Mitome, H., Hatanaka, S.-I., 2002. Optimization of a sonochemical reactor using a pulsing operation. Ultrasonics 40, 683–687.

Mohamad, M., Ali, M., Ahmad, A., 2010. Modelling the extraction of major phytochemical components from *Eurycoma longifolia*. J. Appl. Sci. 10, 2572–2577.

Mohamad, M., Ali, M.W., Ripin, A., Ahmad, A., 2013. Effect of extraction process parameters on the yield of bioactive compounds from the roots of *Eurycoma longifolia*. J. Teknol. 60, 51–57.

Mohamed, A.N., Vejayan, J., Yusoff, M.M., 2015. Review on *Eurycoma longifolia* pharmacological and phytochemical properties. J. Appl. Sci. 15, 831.

Mohd Effendy, N., Mohamed, N., Muhammad, N., Naina Mohamad, I., Shuid, A.N., 2012. *Eurycoma longifolia*: medicinal plant in the prevention and treatment of male osteoporosis due to androgen deficiency. Evidence Based Complement. Alternat. Med. 2012, 125761.

Mohd Zaki, A., Nor Fadilah, W., Mohd Radzi, A., Sui, K.L., Mohamad Lokmal, N., Abdul Rashid, L., Fauzi, A., Fazwa, F., Regina Mariah, J., 2015. Preliminary phytochemical screening of eurycomanone for selection of high quality planting materials: *Eurycoma longifolia*. Malaysian Appl. Biol. 44, 25–29.

Montante, G., Bakker, A., Paglianti, A., Magelli, F., 2006. Effect of the shaft eccentricity on the hydrodynamics of unbaffled stirred tanks. Chem. Eng. Sci. 61, 2807–2814.

Myers, R.H., Montgomery, D.C., Anderson-Cook, C.M., 2016. In: Response Surface Methodology: Process and Product Optimization Using Designed Experiments. John Wiley & Sons, Hoboken, New Jersey, p. 828.

Nordin, M., 2014. Distribution of the population of Tongkat Ali (*Eurycoma* spp.) in Malaysia based on data taken from herbarium records. Med. Aromat. Plants 3, 155.

Nurhanan, M., Asiah, O., Rafedah, A., Mohd Ilham, A., Anee Suryani, S., Mohd Radzi, A., 2004. Protein and chemical fingerprints of different plant parts of E. longifolia. In: Poster presented at the 3rd MMBPP Symposium, pp. 27–28.

Pace, C.N., Trevino, S., Prabhakaran, E., Scholtz, J.M., 2004. Protein structure, stability and solubility in water and other solvents. Philos. Trans. R. Soc. London, Ser. B 359, 1225–1235.

Park, S., Nguyen Xuan, N., Phan Van, K., Chau Van, M., Bui Huu, T., Kim, N., Yoo, H.H., Song, J.-H., Ko, H.-J., Kim, S.H., 2014. Five new quassinoids and cytotoxic constituents from the roots of *Eurycoma longifolia*. Bioorg. Med. Chem. Lett. 24, 3835–3840.

Pingret, D., Fabiano-Tixier, A.-S., Le Bourvellec, C., Renard, C.M., Chemat, F., 2012. Lab and pilot-scale ultrasound-assisted water extraction of polyphenols from apple pomace. J. Food Eng. 111, 73–81.

Pingret, D., Tixier-Fabiano, A., Chemat, F., 2013. Ultrasound-assisted extraction. In: Rostagno, M.A., Prado, J.M. (Eds.), Natural Product Extraction: Principles and Applications. Royal Society of Chemistry, UK, pp. 89–112.

Preece, K.E., Hooshyar, N., Krijgsman, A., Fryer, P.J., Zuidam, N.J., 2016. Intensified soy protein extraction by ultrasound. Chem. Eng. Process. Process Intensif.

Preece, K.E., Hooshyar, N., Krijgsman, A., Fryer, P.J., Zuidam, N.J., 2017. Intensified soy protein extraction by ultrasound. Chem. Eng. Process. Process Intensif. 113, 94–101.

Raso, J., Manas, P., Pagan, R., Sala, F.J., 1999. Influence of different factors on the output power transferred into medium by ultrasound. Ultrason. Sonochem. 5, 157–162.

Rinas, A., Jones, L.M., 2015. Fast photochemical oxidation of proteins coupled to multidimensional protein identification technology (MudPIT): expanding footprinting strategies to complex systems. J. Am. Soc. Mass Spectrom. 26, 540–546.

Rombaut, N., Tixier, A.S., Bily, A., Chemat, F., 2014. Green extraction processes of natural products as tools for biorefinery. Biofuels, Bioprod. Biorefin. 8, 530–544.

Roselló-Soto, E., Barba, F.J., Parniakov, O., Galanakis, C.M., Lebovka, N., Grimi, N., Vorobiev, E., 2015. High voltage electrical discharges, pulsed electric field, and ultrasound assisted extraction of protein and phenolic compounds from olive kernel. Food Bioprocess Technol. 8, 885–894.

Russin, T.A., Arcand, Y., Boye, J.I., 2007. Particle size effect on soy protein isolate extraction. J. Food Process. Preserv. 31, 308–319.

Sališová, M., Toma, Š., Mason, T., 1997. Comparison of conventional and ultrasonically assisted extractions of pharmaceutically active compounds from *Salvia officinalis*. Ultrason. Sonochem. 4, 131–134.

Samaram, S., Mirhosseini, H., Tan, C.P., Ghazali, H.M., Bordbar, S., Serjouie, A., 2015. Optimisation of ultrasound-assisted extraction of oil from papaya seed by response surface methodology: oil recovery, radical scavenging antioxidant activity, and oxidation stability. Food Chem. 172, 7–17.

Santos, H.M., Lodeiro, C., Capelo-Martínez, J.L., 2009. Power ultrasound. In: Capelo-Martínez, J.L. (Ed.), Ultrasound in Chemistry: Analytical Applications. Wiley, Darmstadt, Germany, pp. 1–16.

Seidel, V., 2012. Initial and bulk extraction of natural products isolation. In: Sarker, S.D., Nahar, L. (Eds.), Natural Products Isolation. Springer, New York, pp. 27–41.

Shirsath, S.R., Sonawane, S.H., Gogate, P.R., 2012. Intensification of extraction of natural products using ultrasonic irradiations A review of current status. Chem. Eng. Process. 53, 10–23.

Shuid, A.N., El-arabi, E., Effendy, N.M., Razak, H.S., Muhammad, N., Mohamed, N., Soelaiman, I.N., 2012. *Eurycoma longifolia* upregulates osteoprotegerin gene expression in androgen- deficient osteoporosis rat model. BMC Complement. Altern. Med. 12, 152.

Sicaire, A.-G., Vian, M.A., Fine, F., Carré, P., Tostain, S., Chemat, F., 2016. Ultrasound induced green solvent extraction of oil from oleaginous seeds. Ultrason. Sonochem. 31, 319–329.

Sousa, A.D., Maia, A.I.V., Rodrigues, T.H.S., Canuto, K.M., Ribeiro, P.R.V., Pereira, R.D. C.A., Vieira, R.F., de Brito, E.S., 2016. Ultrasound-assisted and pressurized liquid extraction of phenolic compounds from *Phyllanthus amarus* and its composition evaluation by UPLC-QTOF. Ind. Crop. Prod. 79, 91–103.

Spigno, G., Tramelli, L., De Faveri, D.M., 2007. Effects of extraction time, temperature and solvent on concentration and antioxidant activity of grape marc phenolics. J. Food Eng. 81, 200–208.

Stamatopoulos, K., Chatzilazarou, A., Katsoyannos, E., 2013. Optimization of multistage extraction of olive leaves for recovery of phenolic compounds at moderated temperatures and short extraction times. Foods 3, 66–81.

Taraba, B., Duehring, S., Španielka, J., Hajdu, Š., 2012. Effect of agitation work on heat transfer during cooling in oil isorapid 277HM. Stroj. Vesn.- J. Mech. Eng. 58, 102–106.

Tazi, L.M., Jayawickreme, S., 2016. Determination of residual dextran sulfate in protein products by SEC–HPLC. J. Chromatogr. B 1011, 89–93.

Tiwari, B.K., 2015. Ultrasound: a clean, green extraction technology. TrAC. Trends Anal. Chem. 71, 100–109.

Toma, M., Vinatoru, M., Paniwnyk, L., Mason, T., 2001. Investigation of the effects of ultrasound on vegetal tissues during solvent extraction. Ultrason. Sonochem. 8, 137–142.

Varzakas, T., Tzia, C., 2014. Food Engineering Handbook: Food Process Engineering. CRC Press.

Veillet, S., Tomao, V., Chemat, F., 2010. Ultrasound assisted maceration: an original procedure for direct aromatisation of olive oil with basil. Food Chem. 123, 905–911.

Vejayan, J., Iman, V., Foong, S.-L., Ibrahim, H., 2013. Protein markers useful in authenticating *Eurycoma longifolia* contained herbal aphrodisiac products. Malaysian J. Sci. 32, 15–23.

Vinatoru, M., 2001. An overview of the ultrasonically assisted extraction of bioactive principles from herbs. Ultrason. Sonochem. 8, 303–313.

Wahab, N.A., Mokhtar, N.M., Halim, W.N., Das, S., 2010. The effect of *Eurycoma longifolia* Jack on spermatogenesis in estrogen-treated rats. Clinics (Sao Paulo) 65, 93–98.

Wang, J.-Y., Yang, Y.-L., Tang, X.-Z., Ni, W.-X., Zhou, L., 2017. Effects of pulsed ultrasound on rheological and structural properties of chicken myofibrillar protein. Ultrason. Sonochem. 38, 225–233.

Wang, L., Weller, C.L., 2006. Recent advances in extraction of nutraceuticals from plants. Trends Food Sci. Technol. 17, 300–312.

Waterborg, J.H., 2009. The Lowry method for protein quantitation. The protein protocols handbook. pp. 7–10.

Xu, Y., Pan, S., 2013. Effects of various factors of ultrasonic treatment on the extraction yield of all-trans-lycopene from red grapefruit (*Citrus paradise* Macf.). Ultrason. Sonochem. 20, 1026–1032.

Yu, X., Gouyo, T., Grimi, N., Bals, O., Vorobiev, E., 2016. Ultrasound enhanced aqueous extraction from rapeseed green biomass for polyphenol and protein valorization. C.R. Chim. 19, 766–777.